International Journal of
Automotive Manufacturing and Materials（IJAMM）

Scilight

Article

Failure Analysis and Reliability Optimization Approaches for Particulate Filter of Diesel Engine after-Treatment System

Dongsheng Zhang [1,2], Minglong Li [2], Liguang Li [1,*], Jun Deng [1], Ye Li [3], Rongfang Zhou [3], and Long Ma [1]

[1] School of Automotive Studies, Tongji University, Shanghai 201804, China
[2] Perkins Small Engines (Wuxi) Co., Ltd., Wuxi 214001, China
[3] Perkins Power Systems Technology (Wuxi) Co., Ltd., Wuxi 214001, China
* Correspondence: liguang@tongji.edu.cn
Received: 20 September 2024; Revised: 10 December 2024; Accepted: 14 January 2025; Published: 14 February 2025

Abstract: Diesel particulate filter (DPF) clogging and high temperature failures are predominant issues affecting the reliability of diesel engines in the market applications. These failures, which include substrate crack and melting, can lead to a significant increment of tailpipe particulate matter (PM) emissions, even exceeding the acceptable limits. Such DPF events not only diminish the vehicle productivity but also escalate the maintenance costs. The DPF, situated downstream in the diesel engine exhaust system, is directly influenced by the health state of the upstream engine and diesel oxidation catalyst (DOC). Addressing the risks of DPF system failures is a complex systems engineering challenge. This paper employs a fault tree analysis (FTA) to identify the root causes of these failures, considering the DPF after-treatment functions, all elements affecting system performance, and key interconnections among these elements. Then the DPF reliability optimization strategies are discussed from a system optimization perspective, focusing on reducing the engine-out PM, ensuring the appropriate substrate volume and precious metal coating content for DPF clogging, improving the virtual DPF soot loading sensor accuracy, lowering the extremely uneven flow or DPF soot loading and adopting the conservative regeneration control for high temperature failures. These measures are crucial to mitigate the failure risks and ensure the reliable DPF operation. To achieve the tighter PN requirement of future regulation, additional DPF optimizations would be required. Adopting the new Cordierite material with a higher porosity, further smaller mean pore size and uniform pore size distribution are one of current developing tendencies from existing studies. The Cordierite material with membrane design would be a new developing direction for further improving of filtration efficiency and better hysteresis of DPF pressure drop, plus lower porosity and thicker wall design would get better robustness and DPF pressure drop.

Keywords: failure analysis; reliability optimization; approaches; diesel engine; DPF

1. Introduction

Since 2020, to meet the increasingly stringent emission requirements of the PM mass and the particulate number (PN), the wall flow DPF devices have been widely employed in China for on road heavy-duty Stage VI and non-road Stage IV diesel engines in the market. Concurrently, to address NO_x emissions, the manufacturers generally adopt technology pathway that includes the electronically controlled high-pressure common rail, the exhaust gas turbocharger, the high pressure exhaust gas re-circulation (EGR), DOC, DPF, selective catalytic reduction (SCR) and ammonia slip catalyst (ASC). For non-road China stage IV engines in the 56~130 kW range, the SCR and ASC are often not integrated due to relatively high tailpipe cycle NO_x

emission limit (3.3 g/kW·h) set by regulations.

A variety of typical failure modes have been seen during the market application of the DPF product, such as DPF clogging, and DPF crack/melting caused by extremely high temperature [1,2].

The diagnostics for DPF clogging failure are mandated by both on road heavy-duty stage VI and non-road stage IV regulations in China. And there are below requirements on road heavy-duty stage VI regulation in China: (1) on-board diagnostic (OBD) of DPF low PM mass filtration efficiency; (2) real-road PN emission supervision with the portable emissions measurement system (PEMS) for in-use vehicles [3,4].

DPF clogging failure can trigger the faulty codes, torque de-rate inducement, and even in-situ or service regeneration requests [5], adversely affecting vehicle usage rates, productivity, and increasing the maintenance costs for both end users and manufacturers. High temperatures failures of the DPF would render the PM trapping efficiency ineffective, leading to a substantial increase in DPF outlet PM emissions.

Cai et al. [6] observed that PN emissions from DPF with high temperature failures can reach to ~10 times of China on road heavy-duty stage VI regulation limit. These high temperature failures are irreversible, typically requiring the displacement of the entire failed DPF substrate, and thus, the maintainable process is costly.

Solving the issues of the DPF clogging and high temperature failures is a critical challenge in the process of product development and usage. Reducing the failure rate of vehicles in the market is the key to improving the vehicles productivity and customer satisfaction. This paper employs a fault tree analysis to identify the root causes of these failures, and focuses on countermeasures to address these issues. The relevant papers that represent current status and progress of research in this area are leveraged to elaborate the failure analysis and countermeasures.

Moreover, the more stringent PN emissions supervision (on 23 nm → 10 nm diameter particle) would be required as one of challenges from future tighter emission regulations [7]. The relevant DPF design that can fulfill the tight PN requirements will be discussed with the combination of this DPF reliability study.

This paper is also elaborated from system engineering perspective, which covers below contents in next section: (1) the DPF after-treatment system function: PM filtration and soot regeneration; (2) all elements affecting the DPF system performance: the engine, DOC, DPF, additional boundary influence factors for the matched type of vehicle, as well as the diesel fuel and oil used by end users; (3) key interconnections among these elements, especially for virtual DPF soot loading sensor.

The preceding papers that focused on all aspects of DPF failures analysis (using the principles of FTA and system engineering), countermeasures are rarely found. The main review papers that related to DPF are firstly checked. Typically, these papers only focus on the studies of DOC or DPF component level, but both the diesel engine and DPF failures analysis are not covered from the perspective of system engineering of entire engine level. Zhang et al. [8] introduced the DOC sulfur poisoning, and alleviating measures. Yang et al. [9] described the sulfur position, as well as removal methods and design rationale for sulfur-resistant catalysts. They are not system studies from entire engine level, because the upstream diesel engine is not involved. Zhang et al. [10] introduced the DPF regeneration technologies, but the DPF failures are not covered. Luo et al. [11] presented the DPF regeneration mechanism, but the DPF failures analysis is not involved. E et al. [12] described the soot formation and removal mechanism by the introduction of work principle of engine and DPF, but DPF failures analysis is not covered.

2. Configuration and Work Principle of DPF after-Treatment System

The typical structure for DPF after-treatment system is shown in Figure 1 [13,14]. In order to improve the capability of DPF regeneration, as well as to utilize in-cylinder late post fuel injection control strategy for the DPF active regeneration, the common layout is to place the DOC in front of the DPF [15,16]. Meanwhile, the DPF differential pressure sensor is employed to indirectly measure the DPF soot loading as part of virtual DPF soot loading sensor, which is the most-widely used technology on diesel engines.

The process of DPF soot trapping and regeneration removal is shown in Figure 2. The engine generated PM (most contents as soot) could be continuously accumulated in DPF substrate. When DPF temperature is greater than or equal to a certain threshold, the soot regeneration can occur spontaneously, which is typically named as passive regeneration. When electronic control unit (ECU) recognizes that the amount of DPF soot loading is greater or equal to the calibration threshold or other counter conditions are met, it will trigger and switch to active regeneration control strategy to accelerate the removal of deposited soot in DPF [17].

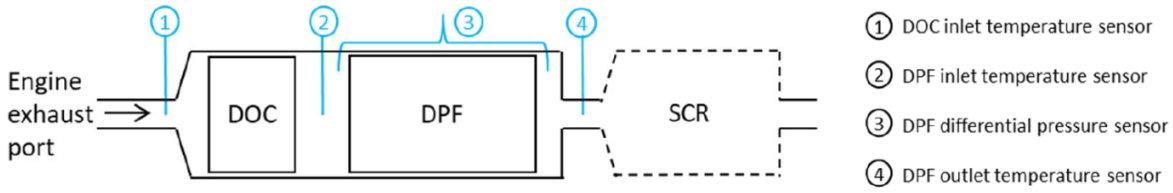

Figure 1. Schematic chart of typical DPF system of diesel engine in the market [13,14].

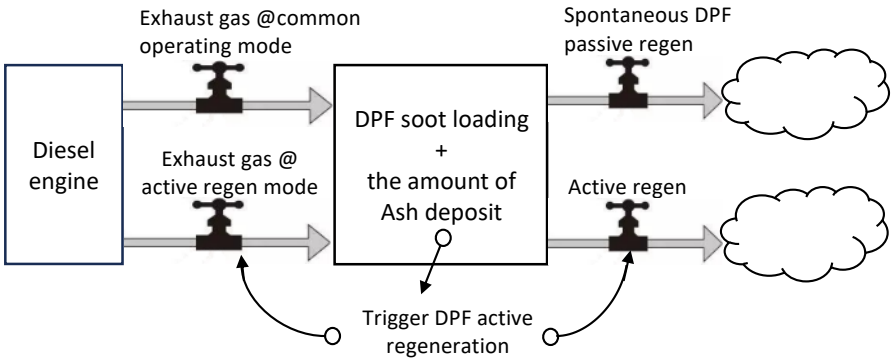

Figure 2. DPF soot trapping and regeneration process.

The ash captured by DPF substrate in the market comes mainly from engine combustion products, such as sulfur, phosphorus, calcium, magnesium, zinc in the engine lubricant oil [18]. Ash continuously deposits in DPF and DOC substrate over time, cannot be fully removed by DPF (active) regeneration, and affects the pressure drop across DPF and virtual DPF soot loading sensor reading [19,20].

The main chemical reactions associated with DPF soot regeneration are shown in Table 1. With the precious metal assistance of DOC (&DPF) coated, the NO that generated by engine combustion can be partially converted into NO_2. Typically, at about 300~350 °C temperature, there is a peak NO conversion ratio ratio. And the oxidation reaction of NO_2 with soot occurs at a lower temperature than that of O_2 with soot, but the former has a much lower soot oxidation removal rate than the latter. Generally, as the exhaust temperature increase, or the amount of precious metal Pt coating increase, or the concentration of NO_2 and O_2 increase, the soot oxidation rate will become higher [21–23]. For DPF active regeneration, the controlled target DOC out temperature is 550~600 °C, and even more (typically < 650 °C) to achieve fast soot removal [24].

Table 1. Main chemical reactions related to soot regeneration [21–23,25].

Chemical Reactions	Temperature Requirements/°C	Determinants of Reaction Rate
$2NO + O_2 \rightarrow 2NO_2$	200~500	temperature, the amount of precious metal coating
$C + 2NO_2 \rightarrow CO_2 + 2NO$	⩾200	temperature, NO_2 concentration
$C + O_2 \rightarrow CO_2$	>460	temperature, O_2 concentration, CDPF (catalyzed DPF) or bare DPF

The above minimum reaction temperature are not fixed values, which are correlated with the amount of the precious metal coating, and concentration of reactors, such as O_2. The temperature values in the Table 1 are reference values from literature [22,23].

3. Selection of Analysis Approach of Root Cause

The common failure analysis methodologies are as follows: (1) fault tree analysis (FTA); (2) fishbone diagram analysis; (3) 5 whys analysis.

The fault tree analysis (FTA) methodology is a top-down deductive approach to identify the root causes

of failures. FTA methodology focuses on the structural breakdown and logical organization of the problem, which is suitable for failure problems analyses of complex system. It is usually used to break down a complex problem into multiple sub-problems to facilitate in-depth, layer-by-layer analysis.

Fishbone diagram analysis methodology is to identify the root causes of failures through the analysis of man, machine, material, method and environment factors. The method would ask a number of participants to take part in a group discussion to brainstorm on all the possible causes of the problem. This method is often used in the area of automotive manufacturing.

5-whys analysis methodology is to trace the root cause of the problem by asking the question "why" on an ongoing basis.

A comparison of these methodologies of failure analysis is summarized in Table 2.

The DPF clogging and high temperature failures are a complex system engineering problem, which involves the engine, DOC, DPF, additional boundary influence factors for the matched type of vehicle, as well as the diesel fuel and oil used by end users. DPF failures can result in PN and PM mass emission exceeding the acceptable limits, which need be reduced to relatively low levels. The FTA analysis method reduces the risk of missing any key individual root causes. Accordingly, FTA approach is a better choice to employ for the DPF failures analysis.

Table 2. Comparison of failure analysis methodologies.

	Pros	Cons	Scope of Application
FTA	Good visualization; can achieve mutually exclusive and collectively exhaustive analysis;	Require professional knowledge and techniques	Suitable for failure problems of complex system, such as the field of aerospace
Fishbone Diagram	Intuitive and easy-to-understand	Insufficiently precise, and influenced by participants' experience and knowledge	Suitable for quality management and various other problem analyses
5-whys	Simple methodology and easy to implement	Require the questioner to have high questioning skills and logical thinking ability	Suitable for situations where a problem needs to be pinpointed quickly

4. Root Cause Analysis of DPF Clogging

The typical DPF substrate materials are Cordierite (Cd) and Silicone Carbide (SiC) for on road heavy-duty and non-road engines, both are ceramic wall-flow filters. And SiC material DPFs are often used on small displacement engines. The safety soot mass/loading limit (SML) is typically limited to 5~6 g/L or less for Cd DPF; the SML is typically around 6~10 g/L for SiC DPF [26–28].

The virtual DPF soot loading sensor readings are often used as one of inputs to trigger DPF clogging faulty code by ECU when soot loading readings are greater than a calibration threshold.

It could be divided into 4 scenarios for both actual DPF soot loading and virtual DPF soot loading sensor reading relationship as below Table 3. For scenario #1 and #2, both would be able to trigger DPF clogging faulty code by ECU. But the scenario #2 indicates a false trip of DPF clogging fault code, which isn't a preferred state.

Table 3. High DPF soot loading scenarios.

Virtual DPF Soot Loading Sensor	Actual DPF Soot Loading: Low	Actual DPF Soot Loading: High
Reading High	#2: High virtual DPF soot loading reading (actual DPF soot loading is overestimated)	#1: High DPF soot loading
Reading Low	#4: NA (low DPF soot loading)	#3: High actual DPF soot loading (actual DPF soot loading is underestimated)

For the scenario #3, there is a high actual DPF soot loading, but virtual DPF soot loading sensor reading is low, which indicates that DPF soot loading is underestimated by virtual sensor. Although there is no DPF clogging faulty code trip, this would result in uncontrolled DPF regeneration and irreversible high DPF temperature failures. Accordingly, the detailed root cause analysis on poor accuracy of virtual DPF soot loading sensor will be covered in next Section 5 for root cause analysis of high temperature failures.

For an extremely large amount of accumulated ash (than expected) in DPF or a sudden collapse of soot layer on CDPF inlet channels, this may result in the virtual DPF soot loading sensor reading from the DPF differential pressure sensor being much higher than actual DPF soot loading [29,30], thereby increasing the false trip risk of DPF clogging fault code to make scenario #2 happen. This types scenario #2 are not the focus of this paper, and will not be covered subsequently.

Accordingly, the next discussion in this Section 4 will focus on root cause analysis of extremely high actual DPF soot loading.

4.1. Engine Generated PM Rate >> Consumption Rate of DPF Passive Regeneration

Under non-active regeneration working mode, when the engine generated PM rate is far greater than the consumption rate of DPF passive regeneration, the DPF soot loading would increase fast. This in return results in extremely high DPF soot loading risk, especially when DPF active regeneration is not timely triggered, or not correctly functioned.

Reducing the calibration setting of active regeneration interval could reduce the extremely high DPF soot loading risks, but could not fully solve this issue. The active regeneration interval is defined by time (hrs) between two times active regeneration, which is calibrated in ECU software [5]. Typically, in order to reduce DPF clogging risk in the market, the active regeneration interval would be appropriately adjusted with the full considerations of the types of vehicles application.

4.1.1. Vehicle Driving Duty Cycle Impacts

For a given DPF after-treatment system design, there are several specific soot loading balance (equilibrium) curves, which consist of the trade-off relationship between NO_x/soot ratio and minimum required DPF substrate temperature, as illustrated in Figure 3. The soot loading balance curve is correlated with the DPF soot loading, as the DPF soot loading increases, the soot loading balance curve moves downward. DPF soot loading does not change when engines operate on the soot loading balance curve [31]. This means that the soot rate generated by the engine is equal to the consumption rate of the DPF passive regeneration.

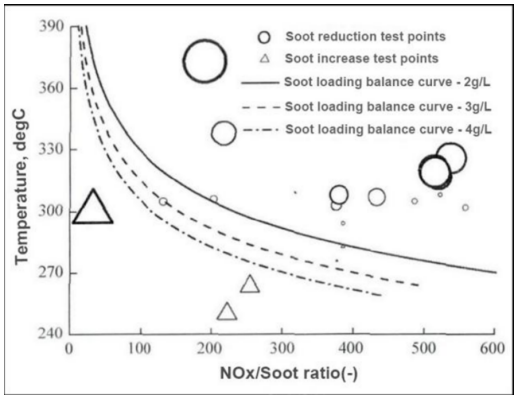

Figure 3. An example of CDPF soot loading balance curve, Reprinted/adapted with permission from [31]. Copyright © 2019, Automotive Engineering.

For a given engine, at each operating point of the engine fuel loop, the engine out emissions and exhaust temperature vary significantly. In general, the engine exhaust temperature decreases as engine load decreases. Meanwhile, in the absence of external loading from vehicle, the engine exhaust temperature generally decreases as the engine speed decreases. Therefore, the capability of DPF passive regeneration is relatively

poor when engine work at low engine loads, such as low idle point.

When engine operates in the above range of soot loading balance curve for most working time, the DPF soot loading would decrease, the engine would be capable to achieve the NO_2-assisted continuous regeneration technology (CRT). Otherwise, the DPF soot loading would increase, and the active regeneration function would be required, even result in much shorter DPF active regeneration interval and extremely high DPF soot loading risk in some extreme circumstances.

For a given type of vehicle in the market, the total engine out NO_x, PM emissions and average exhaust gas temperature are determined by (1) the typical vehicle driving duty cycle, (2) the engine out emissions and exhaust temperature at each engine operating point. The vehicle driving duty cycles could be converted into engine speed, engine loading, and time weighting factors. The engine operating point is defined by engine speed and loading. The typical vehicle driving cycle is defined to represent the majority of end users' driving habits. Between typical driving duty cycles of each types of vehicle, there is a noticeable diversity of average temperatures, for example, excavator with ~360 °C versus wheel loader with ~240 °C from a study [32]. This would lead to a noticeable diversity on DPF passive regeneration capability and soot loading balance point (g/L) between each types of vehicle.

Accordingly, for a given engine (including DPF after-treatment system) design and control, the following scenarios would increase the risk of extremely high DPF soot loading: (1) the typical vehicle driving duty cycle is incorrectly identified; (2) DPF clogging risk level is not sufficiently verified for each vehicle driving duty cycle.

4.1.2. Too high Engine Generated PM Rate

For a given type of vehicle, the typical vehicle driving duty cycle is determined. The engine out NO_x, PM emissions and exhaust temperature are critical boundary condition inputs, which are key contribution factors to determine the risk level of high DPF soot loading in the market application.

At steady state engine operating points, the minimum NO_x/PM ratio development goal setting would be determined by both DOC/DPF hardware design and active regeneration interval target.

Because of well-known trade-off relationship between engine out NO_x and PM emissions, engines with lower engine out NO_x emissions target setting are more likely to have low NO_x/PM ratios.

4.1.2.1. Key Components that Determine Engine Generated PM Rate

In order to meet the development objective of minimum NO_x/PM ratio, it's critical to optimize both key emission components design and combustion relevant calibration settings in ECU.

Typically, the key emission components refer to combustion system, fuel system and intake air system as illustrated in Figure 4.

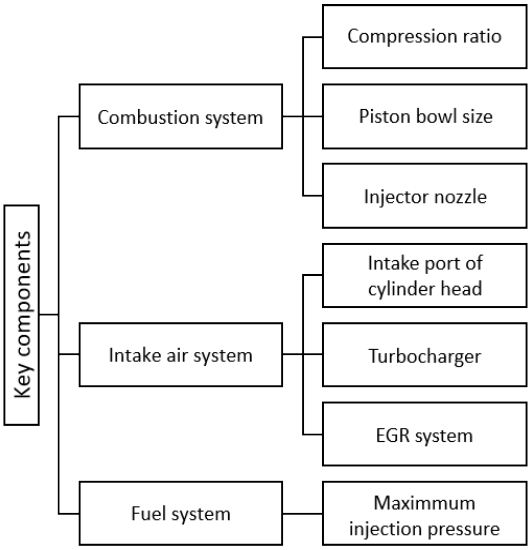

Figure 4. Key emission components.

The combustion relevant calibrations refer to intake manifold pressure, EGR ratio, fuel injection pressure, injection timing at each engine operating points.

4.1.2.2. Engine Generated PM Rate Higher than Normal

For the diesel engines operating under extreme conditions, the typical root causes of high engine out PM are shown in Figure 5.

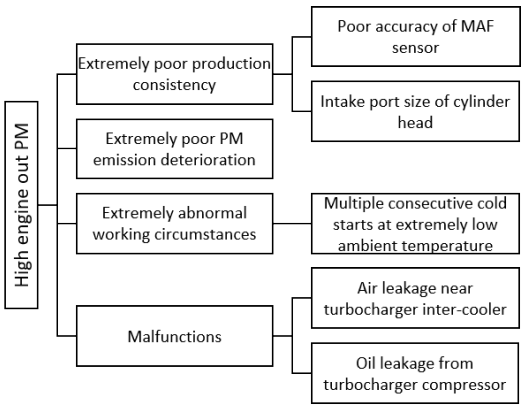

Figure 5. Root causes analysis of high engine out PM.

The main root causes can be divided as below categories: (1) the extremely poor production consistency of key emission components, and the mentioned component is much sensitive to engine out NO_x/PM emissions, such as the poor accuracy of the fresh mass air flow (MAF) sensor [33], excessive deviation of the swirl ratio of cylinder head intake port [34]; (2) the extremely poor PM emission deterioration over vehicle lifetime; (3) extremely abnormal working circumstances, for example, extremely abnormal high density diesel fuel [35], insufficient oxygen concentration in the atmosphere, multiple consecutive cold starts at extremely low ambient temperature; (4) malfunctions that result in low air fuel ratio, such as the low boost pressure caused by air leakage near turbocharger inter-cooler, a large amount of oil abnormally entering the cylinder during a short period of time, or injector hole clogging due to abnormal contamination from low pressure fuel system.

The increment of intake air O_2 content and adding oxygenated fuel blended in diesel could reduce the engine out PM emission [36 – 38]. Conversely, insufficient oxygen concentration in the atmosphere could result in the engine generated PM higher than normal.

Any products would have production variability and durability deterioration, but both require to control in a reasonable range. The sufficient engineering margin would be required to cover the normal product variability and deterioration.

The anomalies examples shown in Figure 5, all can result in the high engine out PM. When these problems happen, the ECU often fail**s** to timely and accurately recognize the high engine out PM, since there is usually no corresponding sensor that can sense above event is occurring, or the recognition process is slow (e.g., low boost pressure failure).

4.1.3. Poor DPF Passive Regeneration Capability

4.1.3.1. Key Designs that Determine DPF Passive Regeneration Capability

As described in Section 4.1.1, for a given DPF after-treatment system design, there are several specific soot loading balance (equilibrium) curves.

The key design that determine DPF passive regeneration capability are as follows: (1) exhaust flow velocity uniformity; (2) precious metal coating; (3) substrate volume. These design optimizations would impact the soot loading balance curves location.

The flow velocity uniformity in front of the DOC and DPF is important for DPF passive regeneration capability, which can be improved by optimizing the design of the upstream pipe (such as diameter, inlet cone

angle). The improved flow velocity uniformity can increase NO conversion efficiency and make DPF soot distribution more even, and thus, improve the total DPF passive regeneration efficiency [39–41].

The amount of precious metal Pt coating (g/L), as well as the DOC substrate volume (L), are ones of the determinants of DOC outlet NO_2 concentration [21, 42]. To achieve the desired DPF passive regeneration capacity, it is required for enough precious metals coating and sufficient DOC volume.

The DPF space velocity increases as DPF volume decreases. The much smaller DPF substrate design will result in insufficient reaction time of NO_2 or O_2 with soot, this in turn gets weak passive regeneration capability. In particular, for CDPF, with identical precious metal coating content (g/L), increasing the carrier CDPF volume can assist in generating more NO_2 to improve the passive regeneration capability.

4.1.3.2. DPF Passive Regeneration Capability Deterioration

For DPF after-treatment system used in the market, the typical root causes of passive regeneration capability deterioration are shown in Figure 6. For the catalyst thermal deactivation, the DOC poisoning and the DOC deposit, all may deteriorate the capability of DPF passive regeneration.

During DPF active regeneration, the controlled target DOC out temperature is 550~650 °C [24]. The temperature inside substrate of DOC and DPF would be much higher. Over the long life cycle of the engine, many DPF active regeneration activities are triggered, deteriorating the Platinum (Pt) catalytic properties as the working time accumulates at high temperatures [43,44]. It may improve the high temperature resistance characteristics through adding a small amount of Palladium (Pd), but it cannot completely solve the problem of catalyst high temperature deactivation (or the thermal sintering) [45]. Catalyst deactivation is permanent, the activity of a high temperature sintered catalyst cannot be restored [46]. Accordingly, the sufficient engineering margins are required to reserve to cover catalyst thermal deactivation impacts.

However, Pd reacts more readily with sulfides from diesel fuel or oil, which can deteriorate the catalytic properties of the precious metal. Sulfur poisoning is typically reversible, at least in part, through DPF active regeneration or other thermal management approaches [42,45].

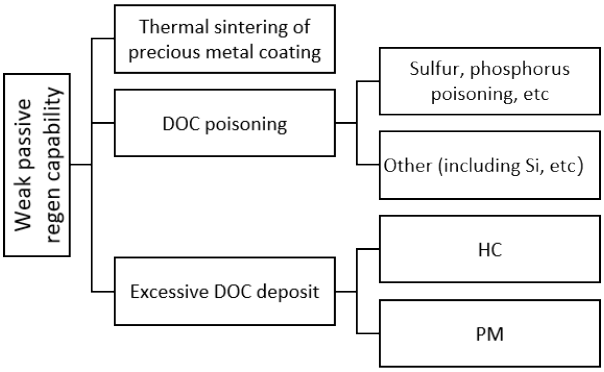

Figure 6. Causes analysis of weak DPF regeneration capability.

As lube oil additives, the phosphorus is another major typical sources of catalyst poisons in diesel exhaust [47 – 49]. The silicon from special working environment or fuel is another uncommon source of catalyst poisons in diesel exhaust gas [46]. The phosphorus and silicon poisoning are almost not able to restore at high temperature (even at 700 °C) [20].

Prohibiting the use of unacceptable diesel fuel and oil is a common way to avoid the occurrence of severe sulfur, phosphorus, and silicon poisoning problems. The allowable fuel and oil are regulated in manufacturer's instruction manual.

Excessive DOC deposit refer to HC and PM, which can cover the surface of DOC wall [50]. It can reduce precious metal catalyst performance by blocking active sites, and thus reduce DPF passive regeneration rate.

The HC is another key main engine out harmful emissions. When engine exhaust temperature is greater than the DOC light off temperature, the HC can be oxidized and removed by catalysis of precious metal. The DOC light off temperature is correlated with the amount of precious metal (catalyst) coating, etc., usually >

200 °C [43,45,51,52]. Especially when the engine operated under low-load conditions for a long period of time, due to the low exhaust temperature (<200 °C), HC and PM are accumulated on DOC to form the "front clogging" and "wall clogging", even form serious face plugging [50,53].

4.2. Unsuccessful DPF Active Regeneration

DPF active regeneration could be activated by (1) virtual DPF soot loading; (2) DPF deltaP reading; (3) the total time since last active regeneration, (4) the total distance since last active regeneration, (5) fuel consumption based [5]. In some circumstances, DPF active regeneration would not be triggered timely, which is one of root cause to drive extremely high DPF soot loading risks.

DPF active regeneration strategy consists of thermal management and/or in-cylinder post hydrocarbon (fuel) injection [17,43,54]. The typical reasons for unsuccessful active regeneration are shown in Figure 7.

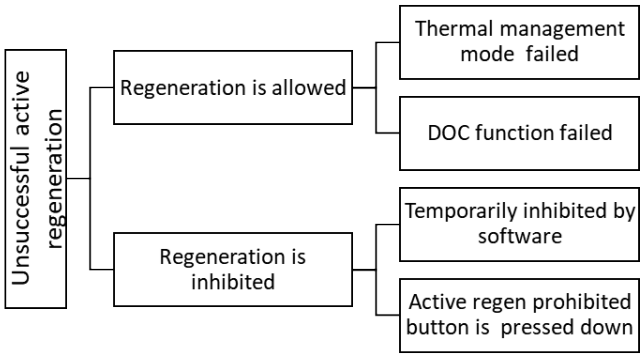

Figure 7. Typical causes of unsuccessful active regeneration.

When the DPF active regeneration strategy is activated, the thermal management mode is firstly functioned to increase the DOC inlet temperature to meet the late post fuel injection precondition in engine cylinder (approximately 300 °C) [17].

The typical root causes that result in thermal management failed are as follows: (1) when the engine runs in specific low speed and low loading zone (such as low idle) for a long period of time, the engine capability is insufficient to raise to the demand temperature by thermal management strategy; (2) the engine hardware failures result in thermal management function failed, such as the mechanical or electronic failures of engine intake throttle valve or exhaust back pressure valve. In the absence of engine component failure, increasing the low idle speed setting is a common practice to improve the effectiveness of thermal management function, especially for DPF in-situ regeneration mode [5].

When the thermal management function meets the requirements, if the DOC conversion efficiency is too low (due to poisoning or DOC face plugging), then the DOC cannot provide the required DPF inlet temperature of DPF active regeneration (≥550 °C, in this case, the low DOC conversion ratio faulty would be triggered). Meanwhile if the engine out PM is too higher at the thermal management mode, this would result in the consistent growth of DPF soot loading and trigger fault code of high soot loading.

When DPF regeneration function is inhibited, it also results in unsuccessful active regeneration, and makes DPF soot loading exceeding the limits.

If end users do not perform active regeneration timely that required by the instruction manual, such as the switch of high speed driving condition or in-situ regeneration, the high DPF soot loading and high temperature failure would be exacerbated. Of course, the development objectives of great product would reduce the customer usage limitations.

Based on the above discussion, it is found that there is a system time delay between the activation of active regeneration and the successive DPF active regeneration, which is thermal management time slots. Therefore, in order to reduce the risk of DPF failures, when active regeneration is activated during vehicle operation processes, in most cases, actual DPF soot loading need be much smaller than SML, otherwise the risks of DPF clogging failures would increase.

5. Root Cause Analysis of High Temperature Failures

The high temperature failures refer to both DPF substrate melting and crack, which are typical failure modes of ceramic wall-flow filters. The melting is caused by high maximum temperature. The crack is mainly caused by higher thermal stress [26]. DPF substrate manufacturing and Canning can also result in the DPF crack failures, but this is not the scope of this paper.

Durability against thermal stress is the most important factor for DPF reliability [55]. When the thermal stress exceeds the DPF substrate material strength, then crack will occur in general. The substrate thermal strength is determined by material selection, design, and Canning, even manufacturing variation, and would be deteriorated by fatigue over accumulated active regeneration time [55].

It's well-known that thermal stress in DPF is proportional to the temperature gradient. Typically, the maximum temperature gradient is proportional to the maximum DPF temperature [56]. The maximum temperatures that cause melting are higher than the ones that result in crack for both Cd and SiC material DPF; when DPF internal maximum temperature reach to ~1000 °C [1,23,57], DPF crack failure would occur, then DPF melting would occur with ~1400 °C maximum temperature [21].

The uncontrolled DPF regeneration can easily damage DPF with too fast soot oxidization rate bringing excessive high temperature, which is typical root cause of high temperature failures [57]. The uncontrolled DPF regeneration can refer to active regeneration that activated by ECU and unintentional soot regeneration that caused by extremely high DOC out temperature due to engine malfunction or inappropriate ECU control.

The Drop to idle (DTI) is the most critical engine operating points transition process, which exacerbates the risk of uncontrolled regeneration due to low exhaust gas mass flows and high oxygen content of the exhaust gas [57,58].

The key root causes of uncontrolled regeneration are illustrated in Figure 8.

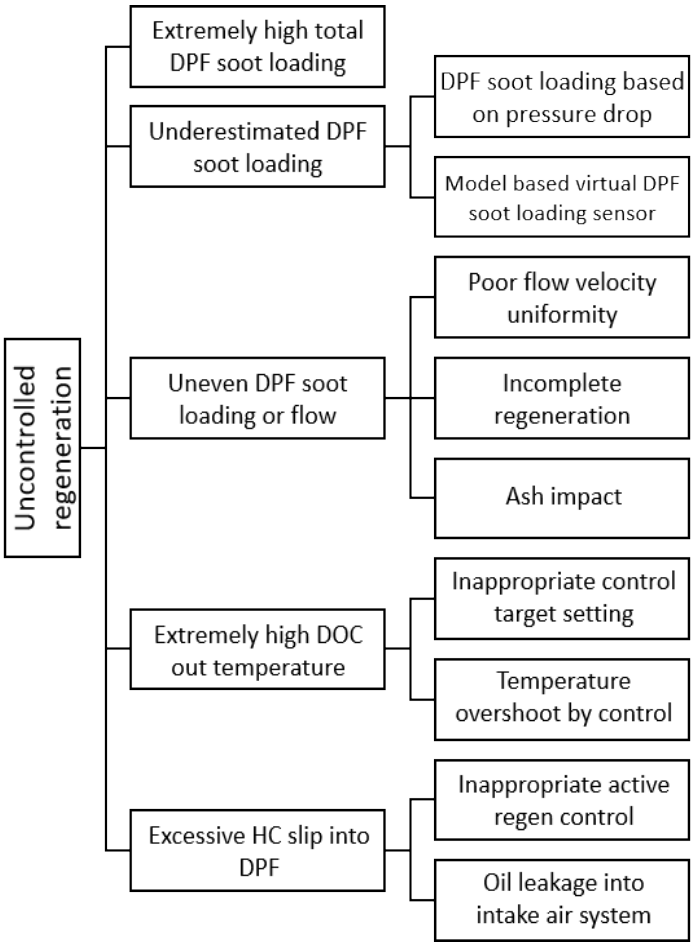

Figure 8. Typical root causes of uncontrolled regeneration.

High total DPF soot loading or uneven local high DPF soot loading are typical root causes of uncontrolled regeneration [57]. And poor accuracy of virtual soot loading sensor can exacerbate the risk of high temperature failures.

Apart from high DPF soot loading, the additional secondary contribution factors of uncontrolled regeneration are as follows: (1) the extremely high DOC out temperature control target setting, for both high temperature ramp up rate at the start of active regeneration and the subsequent flat temperature control target setting; (2) DOC out temperature overshoot against control target due to worse performance of DOC out temperature close loop controller or too much HC accumulated on DOC substrate; (3) excessive HC slip into DPF, etc. [1, 57, 59, 60]. For example, in order to reduce excessive HC slip risk post DOC during active regeneration, the DOC in temperature thresholds of in-cylinder late post start injection are conservatively set through considering extreme work conditions (that mentioned in Section 4.1.3); and the in-cylinder late post injection will be cut off in case of long idle phases (or low DOC in temperature condition) above 150 s [5]. These are not focus of this paper, the sufficient acceptable performance of above 3 items are assumed for subsequent discussion.

5.1. Extremely High DPF Soot Loading

It's well known that the maximum DPF temperature would increase as DPF soot loading increases [61].

The detailed root cause analysis on high DPF soot loading was already summarized in Sections 4.1 and 4.2.

5.2. Poor Accuracy of Virtual Soot Loading Sensor

The virtual DPF soot loading sensor is a critical security to prevent high temperature failures under high actual DPF soot loading conditions.

When high DPF soot loading could be recognized timely, ECU could take a mitigation strategy to reduce the risk of high temperature failure, such as reducing the control target of DOC out temperature [59].

The following is an introduction to the virtual DPF soot loading sensor, specifically why the DPF soot loading may be underestimated.

5.2.1. Virtual Sensor Based on Pressure Drop

The contribution factors of virtual DPF soot loading reading error are firstly summarized as below: (1) relevant sensors tolerance accumulation; (2) DPF pressure too low or pressure slope too shallow over DPF soot loading change; (3) hysteresis effect of DPF pressure drop by incomplete active regeneration; (4) hysteresis effect of DPF pressure drop by NO_2 assisted passive regeneration impact; (5) ash accumulation impact; (6) engine malfunction, for example, intake air leakage, and the engine don't configure sensors to identify the failure timely.

For a given DPF after-treatment system, the DPF soot loading could be calculated based on relationship between exhaust volume flow rate and DPF differential pressure, as illustrated in Figure 9 [62].

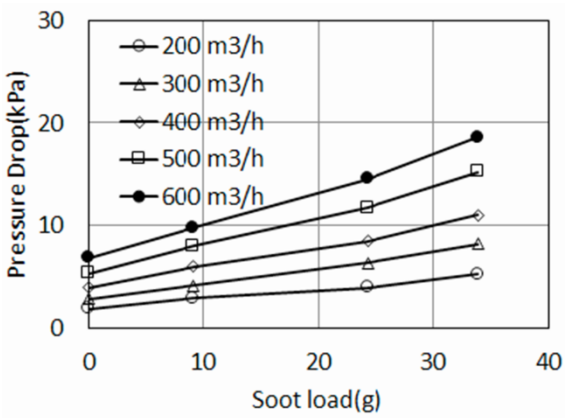

Figure 9. Pressure drop, volumetric flow and DPF soot loading relationship. Reprinted with permission from [62], Copyright © 2018, IFAC (International Federation of Automatic Control).

The accuracy of exhaust mass flow related sensors (such as MAF sensor), DPF differential pressure sensor, DPF temperature sensor will directly affect the calculation accuracy of the virtual DPF soot loading sensor [25,62].

The sensitive relationship between DPF differential pressure and actual DPF soot loading is critical to make this virtual DPF soot loading sensor accuracy acceptable. When DPF differential pressure reading is extremely low, or change rate is too small over soot loading varying, the virtual DPF soot loading sensor accuracy will be worsen [25,54]. The DPF substrate or Canning production variability factors would make the virtual DPF soot loading sensor into more severe condition. In general, below DPF design scenarios would get lower DPF pressure or shallow pressure slope: (1) Cordierite DPF pressure < SiC DPF pressure; (2) low DPF wall thickness; (3) high DPF volume; (4) low substrate length and diameter ratio (L/D); (5) high porosity; (6) asymmetric cell technology (with higher ash capacity) [21,25,63].

The hysteresis effect of DPF differential pressure measurement will deteriorate the accuracy of DPF soot loading estimation. Iwasaki et al. [61] carried out a test on low porosity (%) DPF in order to compare the complete and incomplete regeneration impacts. The test results show that the actual DPF soot loading vary considerably with the identical DPF differential pressure sensor reading, which is known as DPF pressure drop hysteresis effect. The hysteresis effect of DPF pressure drop is caused by the soot distribution location diversity inner DPF substrate between wall pores and DPF channels.

Using optical visualization tool, the study by Choi et al. [64] showed that the NO_2 assisted passive regeneration would preferentially oxidize the soot inner DPF porous wall. Theoretically, it would degrade the accuracy of DPF soot loading estimation, especially for high DPF temperature conditions (such as 400 °C), this is proved by many studies [65,66]. Ran et al. [62] conducted the DPF soot loading estimation accuracy check for both highway driving cycle (with passive regeneration) and city driving cycle, the data demonstrates that the accuracy of the DPF soot loading estimation become worse for high driving cycle, and the DPF soot loading is underestimated during high driving cycle.

In addition, ash can also lead to inaccurate DPF soot loading calculation value based on DPF differential pressure input. Dimou et al. [67] carried out a test on non-catalyzed and 50% porosity DPF. The correlation relationship between DPF soot loading and DPF pressure drop is measured against several ash accumulated levels, the results demonstrate that the actual DPF soot loading values vary noticeably with identical DPF pressure drop. Comparing the data at the 5 g/L and the 0 g/L ash accumulation, under the identical DPF pressure drop condition, the DPF soot loading (for soot loads in excess of 2 g/L area) at 5 g/L ash accumulation is ~2 g/L underestimated than that at 0 g/L ash.

In some extreme circumstances (engine malfunction), when fresh air mass flow recognized by ECU is overestimated or when there is an exhaust gas leakage near DPF inlet, it will result in an underestimation of DPF soot loading identified by ECU. For engine installed a MAF sensor, when there is air leakage near turbocharger air inter-cooler, this is one of example on overestimated fresh air mass flow.

5.2.2. Model Based Virtual DPF Soot Loading Sensor

When engine exhaust flow is very small, the DPF soot loading calculation approach based on DPF pressure drop is not credible [25], a model-based approach to estimating DPF soot loading is required from ECU.

From ECU algorithm, the model based virtual DPF soot loading is calculated as below similar Equation (1):

$$m_{net} = \sum m_{in} - \sum m_{oxidation} \quad (1)$$

where m_{net} is the soot loading in DPF, m_{in} is the engine out soot rate, $m_{oxidation}$ is the soot oxidation rate by the NO_2 and O_2 in DPF [54,68].

The accuracy of the DPF soot loading model would be correlated with the matched vehicle driving duty cycle [63].

As described in Section 4.1.2.2, below scenarios would make the engine generated PM rate higher than normal, such as extremely poor production consistency of key emission components, extremely poor PM emission deterioration, extremely abnormal working circumstances, engine malfunctions. Typically, this model based virtual DPF soot loading sensor could not reflect the real DPF soot loading when above

scenarios happen.

And in many of the extreme scenarios mentioned in Section 4.1.3.2, the anomalies are often not recognized because the corresponding sensors are often not integrated, such as NO_2 concentration sensor post DOC, oxygen sensor before DOC, etc. And thus, the DPF soot loading maybe underestimated in such scenarios.

If all anomalies that mentioned in Sections 4.1.2.2 and 4.1.3.2 can be mitigated with system optimization, the model based virtual DPF soot loading sensor accuracy would be much reliable, even better than virtual DPF soot loading based on pressure drop.

5.3. Uneven DPF Soot Loading or Flow

The uneven soot loading distribution or exhaust flow in DPF is one of main root causes for uncontrolled regeneration to damage DPF [57].

The key contribution factors are as follows: (1) poor flow velocity uniformity; (2) incomplete DPF active regeneration; (3) ash impact.

The poor flow velocity uniformity can result in the excessively high local DPF soot loading. The improving of flow velocity uniformity can make the soot distribution more even in DPF substrate [57]. DOC/DPF substrate face plugging would also drive the poor flow velocity uniformity risk. The root causes of poor flow velocity uniformity and face plugging were already covered in Section 4.1.3.

When active regeneration is incomplete, this would have risk to make local DPF soot loading uneven for next cycle DPF soot accumulation process.

And the local soot distribution in DPF has a strong correlation with the engine operating conditions or vehicle driving duty cycles [69]. The NO_2 assisted passive regeneration would be one of contribution factors, especially for CDPF.

The two boundary ash deposition patterns in DPF are as follows: (1) wall layer and (2) filling at the back end of the inlet channels. In literature mainly two substantially different deposition patterns are described. In one ideal pattern the ash builds a homogeneous layer, covering the DPF wall of the inlet channel. In the other ideal pattern the ash fills the inlet channels from the back of the filter [29].

Many contribution factors influence the observed ash deposition patterns over time on vehicles in the market, such as velocity, regeneration interval, regeneration type, regeneration severity, etc. [29,70]. The uneven ash distribution refer to two aspects: (1) from DPF inlet to outlet, (2) from DPF substrate center line to skin.

Typically, the ash firstly accumulates along the DPF wall channel, then uniformly packs close to the rear end of the DPF (real end filling) for field vehicles. As the ash accumulate to rear end of DPF, the effective volume that accumulate soot will decrease, and uneven soot/ash distribution have risk to occur [71].

The actual ash deposition patterns over time would be better to check from uncontrolled regeneration risk assessment considerations for any new being developed type of vehicle.

Some studies are conducted with ash acceleration test approaches. Zhang et al. [72] conducted active regeneration over the accumulated amount of ash 0 g/L, 5 g/L, 10 g/L, 20 g/L, 40 g/L. As illustrated in Figure 10, with actual 4 g/L soot loading, the test results show that both maximum DPF temperature and maximum temperature gradient increases, which is caused by the decreasing of effective soot deposited volume.

Zhang et al. [72] conducted similar active regeneration tests with constant DPF pressure drop. There is no DPF soot loading correction algorithm in ECU as ash accumulates in this case. When the amount of ash accumulation is 0 g/L, 5 g/L, 10 g/L, 20 g/L, 40 g/L, the actual DPF soot loading is 4 g/L, 4.6 g/L, 3.7 g/L, 3.1 g/L and 1.4 g/L, respectively. As illustrated in Figure 11, the maximum DPF temperature gradient increases to extremely high level (152.5 °C/cm) as ash accumulates (to 40 g/L), which increases the risk of high temperature failure (DPF crack). As ash accumulates to larger level, the local ash/soot and exhaust flow distribution in DPF become significantly uneven from substrate center to skin for tested DPF outlet, as illustrated in Figure 12. This is believed as root cause of above maximum temperature gradient increase.

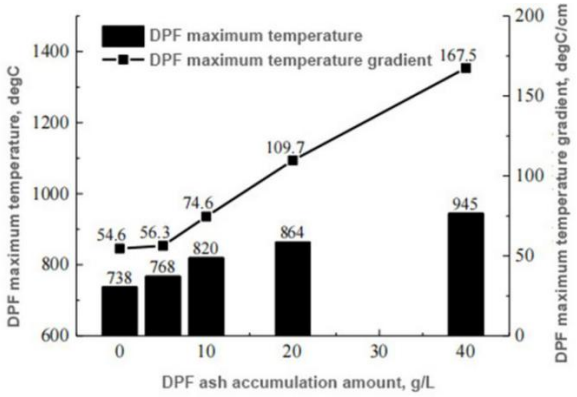

Figure 10. Maximum temperature and temperature gradient over each amount of ash @identical soot loading. Reprinted with permission from [72].

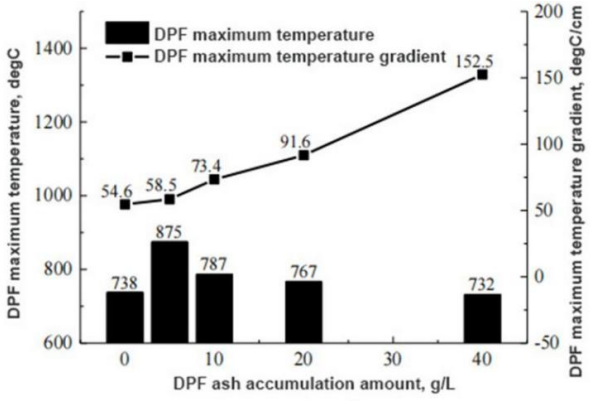

Figure 11. Maximum temperature and temperature gradient over each amount of ash @identical DPF pressure drop. Reprinted with permission from [72].

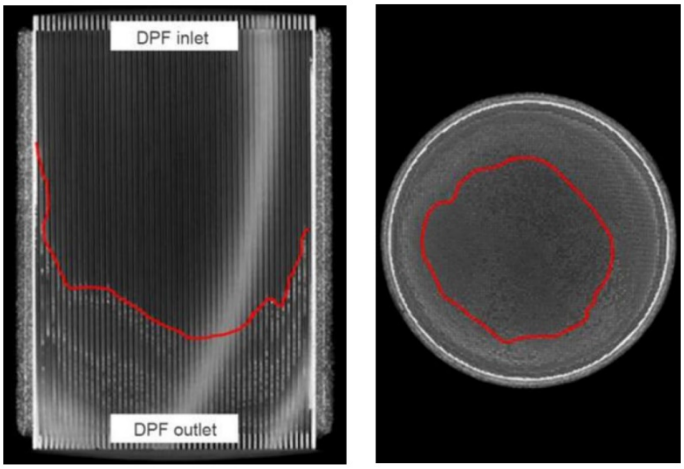

(**a**) cross-section view (**b**) vertical-section view

Figure 12. DPF X-ray CT picture @40 g/L ash loading. Reprinted with permission from [72].

6. Reliability Optimization Approaches

The product reliability is key for manufacturers and end users in market applications, it's critical to improve reliability of particulate filter of diesel engine after-treatment system. The approaches on how to reduce the risks of DPF clogging and the high temperature failure will be elaborated from the point of view of

engine and after-treatment system integration optimization.

The system optimization work will focus on the hardware design, the ECU algorithm and calibration. During optimization process, there are many performance trade-off relationships. These must be used to balance trade-offs to meet customer requirements. In additional, the impacts of normal product production consistency and usage deterioration (PM emission) in the market need be considered as high priority. The sufficient design margin and the conservative regeneration control would be critical to mitigate DPF clogging and high temperature failures risk.

6.1. Optimization of Engine Generated PM Rate

For a given type of vehicle, the optimization of engine out PM is crucial to achieve the engineering objective of active regeneration interval, and reduce the risks of DPF clogging and high temperature failure.

The engine out emissions optimization work consists of combustion development and calibration optimization. The combustion development work is to select the appropriate key emission components that meet the development goals (especially for NO_x/PM ratio) at each engine speed and toque points for a given matched type of vehicle.

Prior to conduct the engine development work, the appropriate engineering development goals (margins) should be set after fully consider the risk associated with the DPF after-treatment capability, normal production consistency, and normal product deterioration factors.

There are stringent emission requirements for both NO_x and PM from regulation. Accordingly, the goal of optimizing engine emissions is often to simultaneously reduce both NO_x and PM (smoke), especially when the engine is not integrated with SCR after-treatment. This means that the emission optimization of engine out is to make the NO_x vs PM (smoke) trade-off line downward, as illustrated example in Figure 13. The 50% variable geometry turbocharger (VGT) position refer to closure percentage. As the VGT closure percentage increases, the intake manifold pressure will increase.

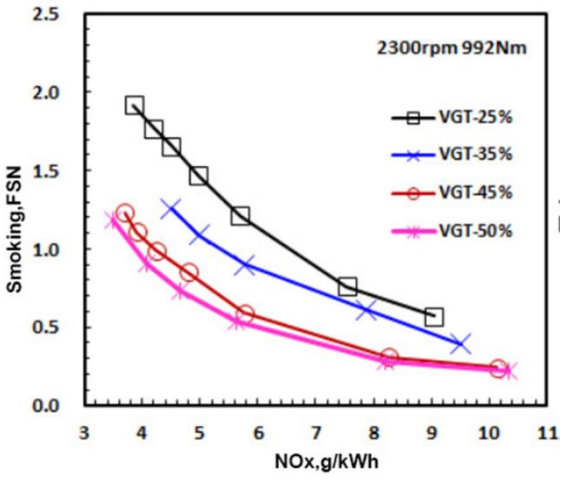

Figure 13. Trade off between NO_x vs PM. Reprinted with permission from [73].

The design of engine piston bowl (combustion chamber) and its matching with injector fuel spray are the ones of most critical factors affecting engine out emissions, which often rely on simulation tool to optimize. And with the upgrading of emission requirements, the design of piston bowl size has the increasing trend of bowl diameter/bowl depth ratio [74,75].

A certain swirl ratio of cylinder head intake port can also promote the air mixing of both air and fuel, and combustion improvement, but if it is too large or too small, it will cause combustion deterioration and emissions increase [34]. As the continuous improving of fuel system injection pressure, the optimal swirl ratio of diesel engine shows a downward trend [76]. Since the swirl ratio and flow coefficient of intake port are negatively correlated, the future cylinder head design trend is to reduce the swirl ratio in order to increase the flow coefficient, which can increase the air fuel ratio and improve combustion.

The additional optimization approaches that can simultaneously reduce both engine out NO_x and PM emissions are summarized in Table 4. The influencing trend summary of these key emission components is on the basis of optimized calibration.

For a 4.5 L non-road diesel engine (rated power: 129.0 kW) with one stage turbocharger, the transient cycle engine out emissions results are as follows: PM is 0.037 g/kW.h, NO_x is 2.62 g/Kw·h [77]. If make the extreme worst assumption that all PM is soot, then the NO_x/PM ratio is 70.8, which suggests that the relative high NO_x/PM ratio is achievable at lower engine out NO_x emissions level. This suggests that it is promising to reduce the risk of failure through engine out emissions optimization even at relatively low NO_x development target settings.

Table 4. Optimization approaches of engine out emissions [73,77–84].

Influencing Factor	Approaches to Simultaneously Reduce NO_x and PM	Adverse Effect
Compression ratio	Appropriately reduce compression ratio [78]	Increase fuel consumption
Injector nozzle parameters	In general, select small static flow or injection hole diameter [77,79]	Increase injector coking risk
EGR cooler efficiency	Improve cooler efficiency [80-82]	Extremely low cooler efficiency increase plugging risk
Turbocharger	Optimize turbocharger efficiency or select two stage turbocharger, and choose a large EGR ratio calibration [83]	Selecting two stage turbocharger will increase cost
Calibration optimization	#1: Increase fuel injection pressure and EGR ratio, select proper injection timing [84] #2: Simultaneously increase boost pressure and EGR ratio [73] #3: Add the appropriate close post injection [84]	Selecting a higher pressure fuel injection system will increase cost

As described in Section 4.1.2.2, the extremely poor engine production consistency and the PM emission deterioration are contribution factors to result in extremely high DPF soot loading. In order to reduce the DPF clogging risk in the market, the manufacturing deviation control, design and control optimization on the key emission components would be required. The extremely abnormal engine working circumstances are contribution factors for extremely high DPF soot loading. Adding the relevant sensors and relevant ECU control algorithm would be capable to reduce the DPF clogging risk that caused by abnormal working circumstances. The details of relevant solutions are not the focus of this paper, will not be expanded.

The engine malfunctions are another contribution factors to result in extremely high DPF soot loading, The relevant solution would be covered in next Section 6.7.

6.2. Optimization of DPF after-Treatment System Integration

The ideal regeneration is the NO_2-assisted continuous regeneration technology (CRT), which do not need perform DPF active regeneration or only need perform fewer DPF active regeneration under extreme special conditions [32]. Therefore the probability of DPF clogging or high temperature failure rate is greatly reduced. But the continuous regeneration DPF system has extremely high requirements on engine out emissions, the type of applied vehicle, and DPF system itself performance. Hence the continuous regeneration DPF system is difficult to realize, especially for some specific vehicle type application with lower average exhaust temperature.

As mentioned in Section 4.1.3.1, the key design that determine DPF passive regeneration capability refers to the velocity uniformity, precious metal coating and substrate volume of DOC/DPF. These design parameters are next optimization work objects. The design optimization working direction is to move the soot loading balance curve (mentioned in Section 4.1.1) downward in order to achieve the product requirements (CRT or active regeneration interval target) and balance the DPF after-treatment cost.

The DPF after-treatment optimization work sequence is shown in Figure 14.

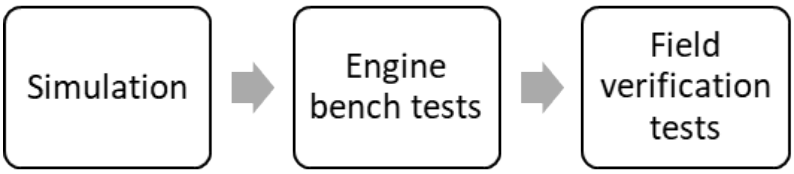

Figure 14. Optimization work sequence.

The CFD simulation can be used to optimize the front pipe of DOC and DPF to improve the substrate inlet velocity uniformity, and this consequently improve the DOC conversion efficiency, the DPF passive regeneration efficiency and local soot distribution uniformity in DPF [39,41].

The numerical model or 1D simulation work can play a key role in the acceptance assessment of high efficiency DOC/DPF emission system integration in the future work [21]. Many studies related to DPF passive regeneration efficiency have been carried out by previous authors. Based on the numerical model, Lee et al. [21] studied both DOC/DPF volume and the amount of precious metal coating effects to the passive regeneration efficiency (or the remaining DF soot loading). Based on the commercial software AVL BOOST v. 5.1., Cordtz et al. [23] conducted the similar study with 1D simulation model, which proved that the model accuracy is good at steady state engine operating points. Based on the Matlab Simulink tool, Bai et al. [22] simulated the passive regeneration efficiency and the remaining DPF soot loading, during 50 or 100 world harmonized transient cycle (WHTC) test, the simulation demonstrates a good accuracy against engine bench test results.

With mentioned above simulation software (or simulation approaches), the design of DOC and DPF (such as substrate volume and precious metal coating) could be optimized, and evaluated if meet the active regeneration interval requirements for a given type of vehicle.

The local soot distribution in DPF has a strong correlation with the engine operating conditions [69]. After above simulation work completed, in order to check if the designed prototype can meet the requirements for the DPF soot loading estimation accuracy, active regeneration interval and DPF active regeneration performance, the engine bench test is firstly required to carry out through simulating the typical driving cycles of a given type of vehicle.

Finally, vehicle field tests are required to verify the fuel adaptability and robustness, such as DPF soot loading accuracy and active regeneration interval [62,85].

The deterioration factors of DPF passive regeneration capability are summarized in Section 4.1.3.2. In order to reduce the DPF clogging risk, the deterioration factors need be taken into consideration for this optimization work.

6.3. Reducing Maximum Regeneration Temperature by DPF Design Optimization

As discussed in Section 5, typically, the maximum DPF temperature during active regeneration could be used to judge the risk level of high temperature failure. The safety DPF soot mass/loading limit (SML) may be defined based on DPF internal maximum temperature during DPF active regeneration under a target controlled DPF in temperature, above of which would damage the DPF. The higher maximum DPF internal temperature indicates a lower allowable SML. The total DPF substrate volume (L) is used to calculate the SML (g/L).

The key DPF design optimization approaches that could reduce maximum DPF regeneration temperature under identical test condition are summarized in Table 5. These design optimization maybe impact the heat loss (temperature drop) over DPF during non-active regeneration mode, this is not focus of this paper, will not be covered.

Table 5. Methodologies to reduce maximum DPF temperature.

Impact Factors	Improving Methodology	Adverse Impacts
Substrate material	Select SiC material as substrate [56,86]	SiC DPF is more expensive than Cordierite DPF,
DPF/CDPF	Select bare DPF (without precious metal coating) [25]	DPF soot regeneration efficiency decreases
Bulk Density	Enhance bulk density [56]	Often leading to an increase of DPF pressure drop
Substrate Porosity (%)	Reduce the DPF porosity [55,61,87,88]	
DPF volume	Reduce DPF substrate volume [86,89]	DPF soot regeneration efficiency decreases
Length/diameter ratio (w/same volume)	Details as below paragraph	NA

Typically, the maximum DPF regeneration temperature of Cordierite is higher than SiC material under the conditions of identical DPF substrate dimension (length/diameter) [75].

A significant improvement in soot oxidation rate could be seen with precious metal coated DPF when compared to bare (uncoated) DPF, which would increase heat release rate and maximum DPF regeneration temperature during active regeneration [25].

Increasing the DPF substrate cell density and wall thickness usually increases the bulk density of DPF filters, which can reduce the maximum DPF temperature during the active regeneration [56].

Reducing DPF porosity has the similar effects with bulk density increase [87]. But both would result in the increment of DPF pressure drop [56,61].

Iwasaki et al. [61] conducted drop to idle comparison tests on both standard and low porosity coated Cordierite DPF, the results show that the low porosity plus thicker wall material could improve the safety soot mass limit (SML) by 2 g/L over the standard material, which is promising.

The lower porosity material plus thicker wall version of the new Cordierite DPF for better robustness is available from the recent paper (2022 year) of key DPF supplier NGK [88].

Miyairi et al. [86] conducted the numerical simulation study on DPF volume impacts to maximum regeneration temperature. Under constant space velocity condition, the results show that maximum DPF regeneration temperature increases as DPF substrate length (or diameter) increases at constant substrate diameter (or length) condition. This mean maximum DPF regeneration temperature increases as the DPF substrate volume increases. In other words, maximum safety DPF soot loading decreases as the DPF substrate volume increases. Kitagawa et al. [89] conducted the real test, revealed the similar conclusion. It's proven that too large volume DPF substrate design would increase the risk of high DPF temperature failure.

DPF substrate length and diameter ratio (L/D) is also one of influencing factors of SML [56]. Lee et al. [90] conducted a simulation study to check the "L/D" impacts on maximum DPF regeneration temperature while maintain the same DPF volume. The results are summarized as follows: (1) for city driving mode (that include drop to idle process), the maximum DPF regeneration temperature increases under the "L/D < 0.6" conditions as "L/D" increases; (2) the maximum DPF regeneration temperature decreases under the "L/D ≥0.6" conditions as "L/D" increases.

6.4. Optimization of Virtual DPF Soot Loading Sensor Accuracy

As described in Section 5, the virtual DPF soot loading sensor is a critical security to prevent high temperature failures under high actual DPF soot loading conditions.

Typically the proposed accuracy is ±1 g/L [68] or ±20% from literature review [5]. In order to achieve the accuracy objective, below optimization on ECU software (including calibration) and hardware are required.

6.4.1. Virtual Sensor Based on Pressure Drop

The key methodologies that can improve virtual DPF soot loading sensor accuracy are firstly summarized as below Table 6.

Table 6. Methodologies to improve DPF soot loading sensor accuracy.

NO.	Resources to Virtual Sensor Error	Methodologies to Reduce Sensor Error
#1	Relevant sensors tolerance accumulation	Select the relative high accuracy sensors
#2	Too lower DPF pressure or shallow pressure slope over soot loading	Improving DPF substrate design (as mentioned factors in Section 5.2.1)
#3	Hysteresis effect of DPF pressure drop by incomplete active regeneration	(1) ECU algorithm and calibration optimization (2) Select high porosity DPF design (plus uniform Pore Size Distribution (PSD)) (3) Selected DPF channel inlet membrane design
#4	Hysteresis effect of DPF pressure drop by NO_2 assisted passive regeneration impacts	
#5	Ash accumulation impact on DPF pressure drop	
#6	Engine malfunction, such as intake air leakage beside inter-cooler	Refer to next Section 6.7

As described in Section 5.2.1, the virtual DPF soot loading sensor with DPF pressure drop principle relies on many physical sensors reading inputs. In order to reduce the accumulation error of virtual DPF soot loading sensor, it would be better to select the high quality (accuracy) physical sensors, especially for DPF pressure drop sensor.

To reduce the underestimated risk of DPF soot loading that causes by hysteresis effect of DPF pressure drop, both ECU software and hardware optimization approaches are available.

From the point of view of ECU software optimization, it would be better to conduct the complete DPF active regeneration timely and regularly. In addition, more sophisticated soot models that considered the NO_2-regeneration impacts are required to improve from some studies [91].

From the point of view of hardware optimization, below two options are available from DPF suppliers: (1) select the high porosity DPF design, (2) select the DPF channel inlet membrane design.

The new Cordierite material was studied by NGK. The hysteresis effect of DPF pressure drop could be reduced with high porosity DPF design plus uniform Pore Size Distribution (PSD) for better virtual DPF soot loading sensor accuracy. And further study would be conducted to check if can achieve the higher PN and PM filtration performance requirements of future tighter heavy duty vehicle and non-road engine emission regulation by together applying smaller Mean Pore Size (MPS) DPF design [88].

Both the NGK and Ibiden company engineers studies indicate that adding the inlet membrane or filtration layer along the DPF channels can get better hysteresis of DPF pressure drop, and improve filtration efficiency [61,92,93]. Now, the technology has been partly used in China on road stage VI applications.

It was not seen yet from literature review if the membrane technology can meet the tighter PN emission requirements of future diesel engine emission regulation. But from study on gasoline particulate filter, NGK expects to be able to achieve Euro7 with membrane technology with Cordierite substrate plug SiC membrane material [94]. Accordingly, the DPF substrate material with inlet membrane would be one of future research directions to achieve the tighter PN emission of future diesel engine regulation.

As described in Section 6.3, the high porosity design would worsen DPF robustness. Therefore, the inlet membrane design plus low porosity and thicker wall would be better solution from DPF product reliability consideration. Meanwhile, the inlet membrane or filtration layer design could reduce the increment level of the DPF pressure drop associated with a low porosity DPF [61].

To reduce the underestimated risk of DPF soot loading over ash accumulation in DPF, both ECU software and hardware optimization approaches are available.

The amount of accumulated ash in the DPF can be estimated through estimates of engine oil consumption or DPF back pressure measurements following complete regeneration [18, 43, 95]. In turn, through the estimation of accumulated ash quantity, the accuracy of DPF soot loading calculated by the ECU can be improved accordingly. But this would not be able to cover the abnormal oil consumption scenarios.

Dimou et al. [67] conducted a comparison tests on 40%, 50% and 60% porosity DPF against several ash accumulated levels, respectively. The results show that with the increment of DPF porosity, the underestimation risk of DPF soot loading over the increment of ash accumulation is reduced. With 60% porosity DPF, under the identical DPF pressure drop condition, the maximum DPF soot loading deviation is

heavily reduced to ~0.5 g/L compared with data over 0~20 g/L ash accumulation in DPF.

As described in Section 5.2.1, with 50% porosity DPF design, there is a underestimated risk of DPF soot loading as ash accumulates in DPF. This is due to the formation of ash cake layer as the ash accumulates over time. The ash cake layer could cover the surfaces pore of substrate wall, prevent soot from entering the pores, reduce the initial soot depth filtration state and accelerate the build-up of a soot cake layer [96].

It was not seen yet from literature review if the lower (40% and 50%) porosity material with inlet membrane can reduce the underestimated risk of DPF soot loading as ash accumulates in DPF. But in theory, the answer would be capable. Because the inlet membrane design could achieve the similar function of ash layer.

6.4.2. Model Based Virtual Soot Loading Sensor

As described in Section 5.2.2, the model based virtual DPF soot loading sensor could not reflect the real DPF soot loading when below scenarios happen: (1) extremely poor production consistency of key emission components, (2) extremely poor PM emission deterioration, (3) extremely abnormal working circumstances, (4) engine malfunctions.

And the DPF soot loading would be also underestimated when DOC poisoning or Excessive DOC deposit.

When above scenarios happen, the virtual sensor based on pressure drop would be more reliable.

6.5. Lowering the Risk of Uneven Soot Loading or Flow

As described in Section 5.3, the key contribution factors on uneven local DPF soot loading or flow are as follows: (1) poor flow velocity uniformity; (2) incomplete DPF active regeneration; (3) ash impact.

The approaches to reduce uneven local DPF soot loading risk are elaborated as below.

The optimization of DOC and DPF inlet dimension design can improve the flow velocity uniformity and the distribution uniformity of soot loading within DPF [39].

DOC/DPF face plugging would also drive the poor flow velocity uniformity risk, the effective ways to mitigate DPF face plugging risks are as follows: (1) optimize the calibration to reduce the engine out HC and PM emissions in the low-load engine operating region; (2) select suitable DOC design, such as appropriate catalyst coating content, too high precious metal coating correlated with increased face plugging risk from test data, and relative lower cell density [97]; (3) carry out the timely and effective thermal management [43]; (4) add another close-coupled DOC near turbo outlet [53].

Incomplete active regeneration is one of contribution factors to make local DPF soot loading uneven for next cycle DPF soot accumulation process. The prolonged active regeneration can reduce this risk, but would drive fuel consumption and oil dilution risk increase.

Ash could not be fully removed from DPF active regeneration, the ash removal during regular maintenance service is one of typical ways to reduce uneven DPF soot loading or exhaust flow and the risk of high DPF failures.

6.6. Optimization of ECU Calibration to Timely Trigger Regeneration

The high DPF soot loading can lead to the uncontrolled regeneration, and destroy the DPF. Therefore, it is critical to timely trigger regeneration to protect DPF from clogging and high temperature failures.

The methodologies that used to reduce the high temperature failure risk are firstly summarized in Table 7.

Considered the virtual DPF soot loading sensor accuracy tolerance, and the system time delay between the activation of active regeneration and the successive DPF active regeneration (that mentioned in Section 4.2), a appropriate margin of calibration threshold that trigger DPF active regeneration need be reserved in comparison with SML. When the regeneration is triggered, the actual soot loading in DPF would better be much less than SML. The reserved margin is determined by virtual DPF soot loading sensor accuracy capability and system time delay of active regeneration for a given type of vehicle.

And as listed #2 approach in Table 7, the frequency of active regeneration should have a relative increasing trend over regeneration cycle and/or ash amount accumulation. The reasons are as follows.

Table 7. Methodologies to reduce failure risk.

NO.	Approaches List	Reasons
#1	In comparison with SML, reserve a appropriate margin of calibration threshold that trigger DPF active regeneration	(1) Virtual DPF soot loading sensor accuracy tolerance; (2) System time delay between the activation of active regeneration and the successive DPF active regeneration
#2	Over active regeneration cycles and/or ash amount accumulation, increase the frequency of active regeneration	Substrate strength deterioration by fatigue over active regeneration time accumulation
		Effective volume decreasing over ash accumulation
		Soot distribution probably become uneven over ash accumulation

When thermal stress is more than DPF substrate strength, DPF fracture failure would occur. DPF substrate strength deterioration by fatigue is positively correlated with DPF active regeneration cycles [55]. And from point of view of reliability, it's recommended by Yamaguchi et al. [55] that the maximum thermal stress is kept lower than about 30% of the initial Cordierite substrate material strength. Therefore, the frequency of DPF active regeneration should have a increasing trend.

As mentioned in Section 5.3, the accumulated ash over vehicle life time can drive below influences: (1) decrease the effective volume of DPF; (2) Soot/ash distribution or flow probably become uneven. In order to reduce the risk of high temperature failure, the frequency of active regeneration should also have a relative increasing trend [17,28].

In summary, the conservative regeneration interval setting is required to mitigate the risk of DPF high temperature failure. And the most active regeneration would better to trigger based on the total time since last active regeneration, the total distance since last active regeneration, fuel consumption based rather than virtual DPF soot loading sensor. This strategy is already employed for the current generation of trucks application, which is proved by key DPF supplier Corning's study [70].

6.7. Optimization to Reduce DPF High Temperature Failures Risk That Driven by Extreme Catastrophic "Event"

Yang et al. [98] conducted a root cause study of filter failure modes based on analysis of field return DPFs. The event-driven failures appeared to be one of the typical cases of filter failures among all field return DPFs, the catastrophic "events" referred to the DPF upstream engine or component malfunctions.

During the extreme catastrophic "events", such as severe intake air leakage, or the additional malfunction failures that listed in Section 4.1.2.2, some of them can lead to high engine out PM emissions and turbo outlet exhaust temperature (even >550 °C turbo outlet temperature at high engine loading points). This increase the DPF thermal failure risk during uncontrolled regeneration or extreme event driven O_2-assisted regeneration.

In order to reduce the DPF failure risks, below three aspects work are required: (1) optimize or strengthen the design to reduce the probability of catastrophic "events" occurring; (2) optimize the system integration and ECU diagnostic algorithm to timely identify the malfunctions; (3) activate the ECU mitigation control logic to reduce DPF failure risk after ECU identified the malfunctions or high DPF soot loading. This is a too huge topic, will just take examples to introduce.

For above (1) item, in order to effectively solve these problems, for failure modes that are less easy to recognize timely, design enhancements need be made to prevent failures. For example, the design of the intake system pipe and clamps at each connection would be strengthened to ensure that the probability of air leakage failure is extremely low, unless vandalism occurs.

The timeliness and accuracy of the actual DPF soot loading identification by ECU is key to mitigate the risk of DPF higher temperature. The MAF sensor location (at the inlet of turbocharger compressor) is too far away of engine intake manifold, this worsen the timeliness of intake air leakage identification by ECU. As a result, when actual air leakage happen near turbocharger inter-cooler, the underestimation issue of DPF soot loading recognized by ECU (via differential pressure sensor) cannot be identified timely. Therefore, it would be better to select the air mass sensors configuration that much close to engine intake manifold, alternatively

installed the oxygen sensor beside DOC. For specific vehicle type (e.g., low activation frequency of the ECU algorithm based on differential pressure calculations), to further reduce the risk of failure, the redundant radio frequency (RF) sensor can be configured at both ends of the DPF to improve the timeliness and accuracy of the actual DPF soot loading identified by ECU [99]. The RF sensor is already commercialized by some engine manufactures on Cordierite DPF.

After the high DPF soot loading is recognized by ECU, reducing the control target of DOC out temperature can be temporarily used to reduce high DPF temperature failures [59]. As a result of reducing the control target of DOC outlet temperature, the fuel consumption for active regeneration would increase significantly [100,101]. This would also increase fuel consumption and oil dilution risk if frequently use this mitigation strategy. Temporarily increasing engine low idle speed setting by ECM is another option to mitigate high temperatures failures risk [102].

7. Summary

Fault tree analysis approach is a good tool for failure analysis on complex system engineering problems.

This paper summarizes the root causes of DPF clogging and high temperature failures, as well as countermeasures to reduce these failure risks.

The main reasons of the DPF clogging failure are as follows: (1) Engine out generated PM rate >> consumption rate of DPF passive regeneration; (2) the poor accuracy of the virtual DPF soot loading sensor; (3) unsuccessful active regeneration. The details are elaborated in this paper.

Excessive total DPF soot loading (especially when DPF soot loading is underestimated by ECU) and uneven local soot distribution are ones of the main root causes of abnormal high DPF temperature failures during DPF active regeneration.

In order to reduce the risks of DPF clogging and high temperature failures, below system integration optimization could improve DPF reliability in market applications.

Option #1: the engine out PM emissions could be reduced through the engine design and calibration optimization, which is critical to mitigate DPF clogging risk.

◇ Below approaches could be taken, such as the reduction of compression ratio, the reduction of the injector static flow and the injection hole diameter, the increase of fuel injection pressure, the increase of the EGR cooler efficiency, the increase of the intake manifold pressure, and close post injection strategy adding.

◇ The impacts of emission consistency and deterioration of production product need be taken into consideration.

Option #2: ensuring the appropriate DPF after-treatment system substrate volume and precious metal coating contents for DPF clogging risk is crucial to mitigate DPF clogging risk.

◇ During development phase, the simulation work, engine bench tests and field tests are to assess the DPF system integration risk.

Option #3: diminishing the maximum regeneration temperature could be achievable with below DPF design optimization.

◇ SiC material DPF

◇ Non-catalyzed DPF

◇ Higher bulk density substrate material

◇ Lower porosity substrate material

Option #4: improving the accuracy of virtual DPF soot loading sensor is critical to mitigate the risk of high temperature failures.

◇ The ECU algorithm and calibration could be optimized, for example, conducting complete active regeneration regularly.

◇ DPF hardware optimization is required, such as the high porosity DPF material with uniform PSD and smaller MPS, the substrate material with inlet membrane. Both examples could get better hysteresis of DPF pressure drop and filtration efficiency.

Option #5: Lowering the risk of uneven soot loading or flow is critical to mitigate the risk of high temperature failures. Below optimization approaches could be taken.

◇The optimization of DOC and DPF inlet dimension design could be conducted with simulation tool assistance.
◇DOC substrate design and regeneration calibration would be an optimization direction.
◇Timely ash removal is typical way to mitigate risk.

Option #6: adopting conservative regeneration control is critical to reduce high temperature failure risk.

◇ The active regeneration interval setting need be appropriately calibrated with the consideration of the system time delay of DPF active regeneration, the substrate strength deterioration by fatigue and the impacts of the amount of ash accumulation.

Option #7: the DPF failures risk that driven by extreme catastrophic "event" need be mitigated from the optimization of system integration level.

◇ The hardware design need be optimized or strengthened to reduce the probability of catastrophic "events" occurring, such as the design of intake air system pipe and clamps at each connections.
◇ The system integration and ECU diagnostic algorithm need be optimized to timely recognize the engine malfunctions. For example, selecting the air mass flow sensors configuration that much close to engine intake manifold could reduce the risk of underestimated DPF soot loading.
◇ After the catastrophic "events" are recognized, the ECU mitigation control logic need be activated to reduce the risk of DPF failure, such as, reducing the control target of DOC outlet temperature, increasing engine low idle speed.

In addition, the correct diesel fuel and oil that regulated by manufacturer's instruction manual are required to adopt by end user for the risk mitigation of DPF failures.

8. Conclusion and Outlook

DPF clogging and high temperature failures are a complex system engineering problem. The fault tree analysis (FTA) is a better choice to identify the root causes of failures in comparison with fishbone diagram and 5-why analysis methodologies.

The extremely higher total DPF soot loading and uneven soot/ash distribution are typical root causes of the uncontrolled regeneration, resulting in high temperature failures. The risk of DPF clogging and high temperature failures can be minimized through system optimization approaches: (1) reducing the engine out PM; (2) ensuring the appropriate DPF after-treatment system substrate volume and precious metal coating contents for DPF clogging risk; (3) diminishing the maximum regeneration temperature by DPF design optimization; (4) improving the accuracy of virtual DPF soot loading sensor; (5) lowering the risk of uneven DPF soot loading or flow; (6) adopting conservative regeneration control for high temperature failures. These relevant optimization could also reduce the risk of PN emissions exceeding limits of PEMS supervision.

To fulfill the tighter PN requirements of future emission regulation, additional DPF optimizations are required, the next development directions are as follows: (1) adopting the new Cordierite material with higher porosity, further smaller mean pore size and uniform pore size distribution; (2) alternatively, developing the new Cordierite material with inlet membrane, lower porosity and thicker wall. Both would improve the hysteresis of DPF pressure drop for better accuracy of virtual DPF soot loading sensor, and DPF pressure drop. The DPF robustness could be improved with lower porosity material plus thicker wall.

And the sensor technology is crucial for mitigating the failure risks. Adopting the radio frequency (RF) sensor on Cordierite DPF would get better accuracy of total DPF soot loading reading. And the commercialized reliable vehicle on-board sensor that could recognize the severity level of uneven soot/ash distribution is not available in the market, which would be required and to be developed for further DPF reliability improving.

The in-cylinder later post fuel injection strategy is a low cost solution, which is adopted by many manufacturers nowadays. To further mitigate the DPF failures risk in the market, the electric heat catalyst

(EHC) devices would be a choice for mitigating unsuccessful active regeneration risk.

Currently, it is the era of rapid development of artificial intelligence (AI). Through telematics technology transmitting engine ECU data to the data platform, based on big data analysis, the virtual man can remotely guide the end user to carry out the appropriate maintenance work in a timely manner. This can be used to improve the reliability of the DPF, and would be a trend in the future.

Author Contributions: Conceptualization and methodology, L.L., D.Z., M.L., J.D.; Investigation: D.Z., Y.L.; Literature review, D.Z., Y.L., R.Z., L.M.; writing—original draft preparation, D.Z.; writing—review and editing, M.L., L.L., D.Z., J. D., Y.L, R.Z., L.M. All authors have read and agreed to the published version of the manuscript.

Funding: This research received no external funding.

Institutional Review Board Statement: Not applicable.

Informed Consent Statement: Not applicable.

Data Availability: Statement: Not applicable.

Conflicts of Interest: The authors declare no conflict of interest.

Definitions/Abbreviations

AI	Artificial intelligence
ASC	Ammonia slip catalyst
CDPF	Catalyzed diesel engine particulate filter
CRT	Continuous regeneration technology
DOC	Diesel oxidation catalyst
DPF	Diesel engine particulate filter
DTI	Drop to idle
ECU	Engine electronic control unit
EGR	Exhaust gas re-circulation
EHC	Electric heat catalyst
FEM	Finite element method
FTA	Fault tree analysis
MAF	Mass air flow
MPS	Mean Pore Size
OBD	On-board diagnostic
PEMS	Portable emissions measurement system
PM	Particulate matter
PN	Particulate number
PSD	Pore Size Distribution
RF	Radio frequency
SCR	Selective Catalytic Reduction
SiC	Silicone Carbide
SML	Safety soot mass limit
VGT	Variable geometry turbocharger
WHTC	World harmonized transient cycle

References

1. Yang, H.; Xin, X.; Zheng, Z.; Yang, Y.; Liu, B.; Liu, Y.; Liu, B. Fault analysis on ring crack of DPF carrier. *J. Shandong Jiaotong Univ.* **2022**, *30*, 8–13. https://doi.org/10.3969/j.issn.1672-0032.2022.03.002.
2. Gong, H. Analysis of Common Aftertreatment Faults in Diesel Engines. *Agric. Mach. Using Maint.* **2023**, *44*–47.

https://doi.org/10.14031/j.cnki.njwx.2023.07.013.
3. *GB 17691-2018*; Limits and Measurement Methods for Emissions from Diesel Fuelled Heavy-Duty Vehicles (China VI). China Environmental Science Press: Beijing, China, 2018.
4. *HJ 1014-2020*; Emissions Control Technical Requirements of Non-Road Diesel Mobile Machinery. China Environmental Science Press: Beijing, China, 2020.
5. Chaudhari, K.; Kumar, R.; Madhukar, P.; Wolter, M. *The Diesel Particulate Filter Calibration—Challenges and Countermeasures Targeting the Indian Scenario*; SAE*Technical Paper* 2021-26-0189; SAE: Warrendale, PA, USA, 2021. https://doi.org/10.4271/2021-26-0189.
6. Cai, Z.; Yan, F.; Hu, J.; Wu, H.; Wang, M.; Shao, Y.; Li, Z. Influence of the engine drop-to-idle process on regeneration temperature, filtration and morphology characteristics of diesel particulate filters. *Fuel* **2023**, *354*, 129324. https://doi.org/10.1016/j.fuel.2023.129324.
7. European Parliament and of the Council. *Regulation (EU) 2024/1257 of the European Parliament and of the Council*; Official Journal of the European Union: Aberdeen, UK, 2024. Available online: https://eur-lex.europa.eu/eli/reg/2024/1257/oj (accessed on 1 December 2024).
8. Zhang, Z.; Tian, J.; Li, J.; Cao, C.; Wang, S.; Lv, J.; Zheng, W.; Tan, D. The development of diesel oxidation catalysts and the effect of sulfur dioxide on catalysts of metal-based diesel oxidation catalysts: A review. *Fuel Process. Technol.* **2022**, *233*, 107317. https://doi.org/10.1016/j.fuproc.2022.107317.
9. Yang, W.; Gong, J.; Wang, X.; Bao, Z.; Guo, Y.; Wu, Z. A Review on the Impact of SO2 on the Oxidation of NO, Hydrocarbons, and CO in Diesel Emission Control Catalysis. *ACS Catal.* **2021**, *11*, 12446–12468.
10. Zhang, Z.; Dong, R.; Lan, G.; Yuan, T.; Tan, D. Diesel particulate filter regeneration mechanism of modern automobile engines and methods of reducing PM emissions: A review. *Environ. Sci. Pollut. Res.* **2023**, *30*, 39338–39376. https://doi.org/10.1007/s11356-023-25579-4.
11. Luo, J.; Zhang, H.; Liu, Z.; Zhang, Z.; Pan, Y.; Liang, X.; Wu, S.; Xu, H.; Jiang, C. A review of regeneration mechanism and methods for reducing soot emissions from diesel particulate filter in diesel engine. *Environ. Sci. Pollut. Res.* **2023**, *30*, 86556–86597. https://doi.org/10.1007/s11356-023-28405-z.
12. E, J.; Xu, W.; Ma, Y.; Tan, D.; Peng, Q.; Tan, Y.; Chen, L. Soot formation mechanism of modern automobile engines and methods of reducing soot emissions: A review. *Fuel Process. Technol. 2022*, **235**, 107373. https://doi.org/10.1016/j.fuproc.2022.107373.
13. Wang, X.; Cheng, D.; Zhang, J.; Ren, X.; Zhao, S. Analysis on failure characteristics of DPF system of diesel engine. *J. Ordnance Equip. Eng.* **2022**, *43*, 229–234+273.
14. Xue, W.L.; Li ,Y. Research on DPF of Particle Filter for Diesel Engine of Internal Combustion Diesel Forklift Truck. *Intern. Combust. Engine Parts* **2024**, *54*–57. https://doi.org/10.19475/j.cnki.issn1674-957x.2024.09.010.
15. Bao, L.; Wang, J.; Shi, L.; Chen, H. Exhaust Gas After-Treatment Systems for Gasoline and Diesel Vehicles. *Int. J. Automot. Manuf. Mater.* **2022**, *1*, 9. https://doi.org/10.53941/ijamm0101009.
16. Russell, A.; Epling, W.S. Diesel Oxidation Catalysts. *Catal. Rev.* **2011**, *53*, 337–423.
17. Raghu, M. Y.; Rajasekar, S., Sr.; Thavasu, R. K.; Bazeer, M.; Sandeep, S. *Simulation-Based Approach for DPF Calibration to Reduce Overall Development Time with Improved Accuracy and Quality*; SAE Technical Paper 2022-28-0373; SAE: Warrendale, PA, USA, 2022. https://doi.org/10.4271/ 2022-28-0373.
18. Kimura, K.; Lynskey, M.; Corrigan, E.R.; Hickman, D.L.; Wang, J.; Fang, H.L.; Chatterjee, S. *Real World Study of Diesel Particulate Filter Ash Accumulation in Heavy-Duty Diesel Trucks*; SAE Technical Paper 2006-01-3257; SAE: Warrendale, PA, USA, 2006. https://doi.org/10.4271/2006-01-3257.
19. Sappok, A.; Santiago, M.; Vianna, T.; Wong, V. W. *Characteristics and Effects of Ash Accumulation on Diesel Particulate Filter Performance: Rapidly Aged and Field Aged Results*; SAE Technical Paper 2009-01-1086; SAE: Warrendale, PA, USA, 2009. https://doi.org/10.4271/2009-01-1086.
20. Andersson, J.; Antonsson, M.; Eurenius, L.; Olsson, E.; Skoglundh, M. Deactivation of diesel oxidation catalysts: Vehicle- and synthetic aging correlations. *Appl. Catal. B Environ.* **2007**, *72*, 71–81. https://doi.org/10.1016/j.apcatb.2006.10.011.
21. Lee, S.J.; Jeong, S.J.; Kim, W.S.; Lee, C.B. *Numerical Study on the Effect of Geometric Shape of DOC/DPF and Catalyst Loading for NO_2-Assisted Continuous Regeneration*; SAE Technical Paper 2007-24-0101; SAE: Warrendale, PA, USA, 2007. https://doi.org/10.4271/2007-24-0101.
22. Bai, S.Z.; Tang, J.; Wang, G.H. Soot loading estimation model and passive regeneration characteristics of DPF system for heavy-duty engine. *Appl. Therm. Eng.* **2016**, *100*, 1292–1298. https://doi.org/10.1016/j.applthermaleng.2016.02.05.
23. Cordtz, R.; Ivarsson, A.; Schramm, J. *Steady State Investigations of DPF Soot Burn Rates and DPF Modeling*; SAE Technical Paper 2011-24-0181; SAE: Warrendale, PA, USA, 2011. https://doi.org/10.4271/2011-24-0181.
24. Xin, Q. *Diesel Engine System Design*; Woodhead Publishing: Cambridge, UK, 2013; pp. 651–758.
25. Singh, N.; Mandarapu, S. *DPF Soot Estimation Challenges and Mitigation Strategies and Assessment of Available DPF Technologies*; SAE Technical Paper 2013-01-0838; SAE: Warrendale, PA, USA, 2013. https://doi.org/10.4271/2013-01-0838.
26. Majewski, W. DieselNet Technology Guide, Diesel Particulate Filters, Diesel Filter Systems. Available online: https://dieselnet.com/tech/dpf_sys.php (accessed on 1 September 2024).
27. Majewski, W. DieselNet Technology Guide, Diesel Particulate Filters, Wall-Flow Monoliths. Available online: https://dieselnet.com/tech/dpf_wall-flow.php (accessed on 1 September 2024).
28. Sappok, A.; Wong V. Ash Effects on Diesel Particulate Filter Pressure Drop Sensitivity to Soot and Implications for Regeneration Frequency and DPF Control. *SAE Int. J. Fuels Lubr.* **2010**, *3*, 380–396. https://doi.org/10.4271/2010-

01-0811.
29. Dittler, A. *Ash Transport in Diesel Particle Filters*; SAE Technical Paper 2012-01-1732; SAE: Warrendale, PA, USA, 2012. https://doi.org/10.4271/2012-01-1732.
30. Kim, K.; Mital, R.; Higuchi, T.; Chan, S.; Kim, C. H. *An Investigative Study of Sudden Pressure Increase Phenomenon Across the DPF*; SAE Technical Paper 2014-01-1516; SAE: Warrendale, PA, USA, 2014. https://doi.org/10.4271/2014-01-1516.
31. Chu, G.; Wang, G.; Qi, J.; Yang, B.; Shuai, S. Study on Passive Regeneration Characteristics and Regeneration Balance Condition of CDPF. *Automot. Eng.* **2019**, *41*, 1365–1369+1434. https://doi.org/10.19562/j.chinasae.qcgc.2019.012.003.
32. Majewski, W. DieselNet Technology Guide, Diesel Particulate Filters, Diesel Filter Systems, Catalytic Diesel Filters. Available online: https://dieselnet.com/tech/dpf_catalytic.php (accessed on 1 September 2024).
33. Guo, D.; Pan, W.; Zhuang, M.; Li, J.; Zhang, C. Optimization of control strategy of intake flow for CHINA VI diesel engine. *Intern. Combust. Engine Powerpl.* **2022**, *39*, 29–34. https://doi.org/10.19471/j.cnki.1673-6397.2022.03.005.
34. Mao, Y.; Xu, J.; Fu, X.; Yang, H.; Chang, Z. EGR Rate and Swirl Ratio Study on Combustion Characteristics of HPD Diesel Engine. *Intern. Combust. Engines* **2018**, 38–41.
35. Liu, H.; Ma, J.; Dong, F.; Yang, Y.; Liu, X.; Ma, G.; Zheng, Z.; Yao, M. Experimental investigation of the effects of diesel fuel properties on combustion and emissions on a multi-cylinder heavy-duty diesel engine. *Energy Convers. Manag.* **2018**, *171*, 1787–1800. https://doi.org/10.1016/j.enconman.2018.06.089.
36. Wang, Y.; Liu H.; Feng L.; Maes, N.; Fang, T.; Cui, Y.; Yi, W.; Somers, B.; Yao, M. Effects of oxygen enrichment on diesel spray flame soot formation in O_2/Ar atmosphere. *Combust. Flame* **2024**, *260*, 113244. https://doi.org/10.1016/j.combustflame.2023.113244.
37. Chen, B.; Liu, X.; Liu, H.; Wang, H.; Kyritsis, D.C.; Yao, M. Soot reduction effects of the addition of four butanol isomers on partially premixed flames of diesel surrogates. *Combust. Flame* **2017**, *177*, 123–136. https://doi.org/10.1016/j.combustflame.2016.12.012.
38. Zheng, Z.; Li, C.; Liu, H.; Zhang, Y.; Zhong, X.; Yao, M. Experimental study on diesel conventional and low temperature combustion by fueling four isomers of butanol. *Fuel* **2015**, *141*, 109–119. https://doi.org/10.1016/j.fuel.2014.10.053.
39. Zhang, X.; Liu, Y.; Xing, S.; Sun, L. Matching Analysis of Aftertreatment System of Off-road Diesel Engine. *Tract. Farm Transp.* **2022**, *49*, 35–38.
40. Gaiser, G.; Mucha, P. *Prediction of Pressure Drop in Diesel Particulate Filters Considering Ash Deposit and Partial Regenerations*; SAE Technical Paper 2004-01-0158; SAE: Warrendale, PA, USA, 2004. https://doi.org/10.4271/2004-01-0158.
41. Oesterle, J.; Gaiser, G.; Zacke, P. *Homogeneous Loading and Regeneration of Diesel Particulate Filters Using Progressive Spin Elements*; SAE Technical Paper 2004-01-1424; SAE: Warrendale, PA, USA, 2004. https://doi.org/10.4271/2004-01-1424.
42. Price, K.; Ummel, D.; Pauly, T. *A Systematic Evaluation of Sulfur Poisoning and Desulfation Behavior for HD Diesel Oxidation Catalysts*; SAE Technical Paper 2018-01-1262; SAE: Warrendale, PA, USA, 2018. https://doi.org/10.4271/2018-01-1262.
43. Munnannur, A.; Ottinger, N.; Gerald Liu, Z. Thermal Management of Exhaust Aftertreatment for Diesel Engines. In *Handbook of Thermal Management of Engines*; Lakshminarayanan, P.A., Agarwal, A.K., Eds.; Springer: Singapore, 2022. https://doi.org/10.1007/978-981-16-8570-5_2.
44. Kim, J.; Kim, C.; Choung, S.J. Comparison studies on sintering phenomenon of diesel oxidation catalyst depending upon aging conditions. *Catal. Today* **2012**, *185*, 296–301. https://doi.org/10.1016/j.cattod.2011.09.021.
45. Pfeifer, M.; Kögel, M.; Spurk, P.; Jeske, G. *New Platinum/Palladium Based Catalyzed Filter Technologies for Future Passenger Car Applications*; SAE Technical Paper 2007-01-0234; SAE: Warrendale, PA, USA, 2007. https://doi.org/10.4271/2007-01-0234.
46. Majewski, W. DieselNet Technology Guide, Diesel Catalysts, Diesel Oxidation Catalyst. Available online: https://dieselnet.com/tech/cat_doc_deactiv.php (accessed on 1 September 2024).
47. Bodek, K.; Wong, V. *The Effects of Sulfated Ash, Phosphorus and Sulfur on Diesel Aftertreatment Systems—A Review*; SAE Technical Paper 2007-01-1922; SAE: Warrendale, PA, USA, 2007. https://doi.org/10.4271/2007-01-1922.
48. Agote-Arán, M.; Jacobsen, V.V.; Elsener, M.; Schütze, F.W.; Schilling, C.M.; Sridhar, M.; Katsaounis, E.; Kröcher, O.; Alxneit, I.; Ferri D. Thermal Sintering and Phosphorus Poisoning of a Layered Diesel Oxidation Catalyst. *Top. Catal.* **2023**, *66*, 777–786. https://doi.org/10.1007/s11244-022-01752-w.
49. Agote-Arán, M.; Elsener, M.; Schütze, F.W.; Schilling, C.M.; Sridhar, M.; Katsaounis, E.; Kröcher, O.; Ferri, D. On the relevance of P poisoning in real-world DOC aging. *Appl. Catal. B Environ.* **2021**, *291*, 120062. https://doi.org/10.1016/j.apcatb.2021.120062.
50. Friese, K.; Eilts, P.; Lüers, B. *Investigations Regarding Deposit Formation on Diesel Oxidation Catalysts*; SAE Technical Paper 2020-01-1432; SAE: Warrendale, PA, USA, 2020. https://doi.org/10.4271/2020-01-1432.
51. Shakya, B.; Sukumar, B.; López-De Jesús, Y.; Markatou, P. The Effect of Pt: Pd Ratio on Heavy-Duty Diesel Oxidation Catalyst Performance: An Experimental and Modeling Study. *SAE Int. J. Engines* **2015**, *8*, 1271–1282. https://doi.org/10.4271/2015-01-1052.
52. Kato, D.; Okano, H.; Inoue, K.; Nakano, K. Development of DPF regeneration system under all operating conditions for generators. *SAE Int. J. Adv. Curr. Prac. Mobil.* **2023**, *5*, 1719–1725. https://doi.org/10.4271/2022-32-0050.
53. Kumar, A.; Zokoe, R.; Joshi, S.; Kamasamudram K.; Yezerets A. *Reactor System with Diesel Injection Capability for*

DOC Evaluations; SAE Technical Paper 2018-01-0647; SAE: Warrendale, PA, USA, 2018. https://doi.org/10.4271/2018-01-0647.
54. Tiwari, A.; Durve, A.; Barman, J.; Srinivasan, P. *Evaluation of Different Methodologies of Soot Mass Estimation for Optimum Regeneration Interval of Diesel Particulate Filter (DPF)*; SAE Technical Paper 2021-26-0208; SAE: Warrendale, PA, USA, 2021. https://doi.org/10.4271/2021-26-0208.
55. Yamaguchi, S.; Fujii, S.; Kai, R.; Miyazaki, M.; Miyairi, Y.; Miwa, S.; Busch, P. *Design Optimization of Wall Flow Type Catalyzed Cordierite Particulate Filter for Heavy Duty Diesel*; SAE Technical Paper 2005-01-0666; SAE: Warrendale, PA, USA, 2005. https://doi.org/10.4271/2005-01-0666.
56. Li, J.; Mital, R. *Effect of DPF Design Parameters on Fuel Economy and Thermal Durability*; SAE Technical Paper 2012-01-0847; SAE: Warrendale, PA, USA, 2012. https://doi.org/10.4271/2012-01-0847.
57. Zhan, R.; Huang, Y.; Khair M. *Methodologies to Control DPF Uncontrolled Regenerations*; SAE Technical Paper 2006-01-1090; SAE: Warrendale, PA, USA, 2006. https://doi.org/10.4271/2006-01-1090.
58. Recker, P.; Pischinger, S. Thermal Shock Protection for Diesel Particulate Filters. *SAE Int. J. Engines* **2012**, *5*, 112–118. https://doi.org/10.4271/2011-01-2429.
59. Huang, T.; Hu, G.; Guo, F.; Yang, M.; Zhu, Y.; Ran, Y. Experiment of DPF Temperature Control During Thermal Regeneration. *Trans. CSICE* **2020**, *38*, 257–264. https://doi.org/10.16236/j.cnki.nrjxb.202003034.
60. Xie, T.; Gao, C.; Lu, W.; Zhang, S.; Li, L. Development and verification of control strategy for DPF regeneration temperature based on model. *Intern. Combust. Engine Powerpl.* **2022**, *39*, 16–21.
61. Iwasaki, S.; Mizutani, T.; Miyairi, Y.; Yuuki, K.; Makino, M. New Design Concept for Diesel Particulate Filter. *SAE Int. J. Engines* **2011**, *4*, 527–536. https://doi.org/10.4271/2011-01-0603.
62. Ran, Y.; Huang, T.; Zhang, M.; Jing, S.; Zhu, Y. DPF Soot Loading Estimation Strategy Based on Pressure Difference. *IFAC-PapersOnLine* **2018**, *51*, 366–368. https://doi.org/10.1016/j.ifacol.2018.10.075.
63. Rose, D.; Boger, T. *Different Approaches to Soot Estimation as Key Requirement for DPF Applications*; SAE Technical Paper 2009-01-1262; SAE: Warrendale, PA, USA, 2009. https://doi.org/10.4271/2009-01-1262.
64. Choi, S.; Lee, K. *Detailed Investigation of Soot Deposition and Oxidation Characteristics in a Diesel Particulate Filter Using Optical Visualization*; SAE Technical Paper 2013-01-0528; SAE: Warrendale, PA, USA, 2013. https://doi.org/10.4271/2013-01-0528.
65. Voutsi, O.; Tsinoglou, D.; Karamitros, D.; Koltsakis, G. Pressure Drop of Particulate Filters and Correlation with the Deposited Soot for Heavy-Duty Engines. *Adv. Curr. Pract. Mobil.* **2020**, *2*, 692–701. https://doi.org/10.4271/2019-24-0151.
66. Kuki, T.; Miyairi, Y.; Kasai, Y.; Miyazaki, M.; Miwa, S. *Study on Reliability of Wall-Flow Type Diesel Particulate Filter*; SAE Technical Paper 2004-01-0959; SAE: Warrendale, PA, USA, 2004. https://doi.org/10.4271/2004-01-0959.
67. Dimou, I.; Sappok, A.; Wong, V.; Fujii, S.; Sakamoto, H.; Yuuki, K.; Vogt, C.D. *Influence of Material Properties and Pore Design Parameters on Non-Catalyzed Diesel Particulate Filter Performance with Ash Accumulation*; SAE Technical Paper 2012-01-1728; SAE: Warrendale, PA, USA, 2012. https://doi.org/10.4271/2012-01-1728.
68. Huang, T.; Zhu, Y.; Ran, Y.; Zhang, M.; Jing, S. Calibration of a Mass Balance Based Soot Load Estimation Model for Diesel Particulate Filter. *IFAC-PapersOnLine* **2018**, *51*, 362–365. https://doi.org/10.1016/j.ifacol.2018.10.074.
69. Yu, J.; Xing, B.; Gao, L. Comparative Study on Different Soot Accumulation Modes of DPF. *Veh. Engine* **2023**, 39–43. https://doi.org/10.3969/j.issn.1001-2222.2023.01.007.
70. Viswanathan, S.; George, S.; Govindareddy, M.; Heibel, A. *Advanced Diesel Particulate Filter Technologies for Next Generation Exhaust Aftertreatment Systems*; SAE Technical Paper 2020-01-1434; SAE: Warrendale, PA, USA, 2020. https://doi.org/10.4271/2020-01-1434.
71. Liu, Y.; Su, C.; Clerc, J.; Harinath, A.; Rogoski, L. Experimental and Modeling Study of Ash Impact on DPF Backpressure and Regeneration Behaviors. *SAE Int. J. Engines* **2015**, *8*, 1313–1321. https://doi.org/10.4271/2015-01-1063.
72. Zhang, J. Studies on the Mechanisms of Ash Effects on DPF Performance and Its Related Application Issues. Ph.D. Thesis, Tsinghua University, Beijing, China, 2019. https://doi.org/10.27266/d.cnki.gqhau.2019.000178.
73. Cao, S. *Research on Diesel Engine Performance Meeting the National Stage VI Emission Regulation*; Dalian University of Technology: Dalian, China, 2017.
74. Sheng, W.; Jin Lin M.; Yang Y.; Zhao H.; Wang D. Development Direction and Trend of Emission Control of Off-road Diesel Engines (37–130 kW). *Intern. Combust. Engine Parts* **2022**, *91*–93. https://doi.org/10.19475/j.cnki.issn1674-957x.2022.04.029.
75. Wang, P. Optimization of Combustion Process for Diesel Engines of Non-Road Machinery. Master's Thesis, Shandong University, Jinan, China, 2020. https://doi.org/10.27272/d.cnki.gshdu.2020.002191.
76. Tan, X.; Wang, T.; Li, Z.; Li, W.; Tian, H.; Sun, K. Key Technology Development for Efficient-Clean- Reliable Heavy-Duty Diesel Engine. *Trans. CSICE* **2020**, *38*, 385–391. https://doi.org/10.16236/j.cnki.nrjxb.202005050.
77. Guo, J.; Li, F.; Li, J.; Li, J. Development Method of Non-Road CN IV EGR Engine Combustion Test. *Mod. Veh. Power* **2022**, *28*–33. https://doi.org/10.3969/j.issn.1671-5446.2022.04.007.
78. Hannu, J.; Magdi, K. K. DieselNet Technology Guide, Engine Emission & Efficiency Technologies, Combustion Systems. Available online: https://dieselnet.com/tech/engine_combustion.php (accessed on 1 September 2024).
79. Zhang, Z.; Liu, Y.; Wu, B.; Nie, J.; Su, W. Effect of Nozzle Diameter on Combustion and Emissions of a Heavy Duty Diesel Engine. *Trans. CSICE* **2022**, *40*, 97–105. https://doi.org/10.16236/j.cnki.nrjxb.202202012.
80. Federico, M.; Paolo, F.; Marco, G. Analysis of different exhaust gas recirculation architectures for passenger car Diesel engines. *Appl. Energy* **2012**, *98*, 79–91. https://doi.org/10.1016/j.apenergy.2012.02.081.
81. Zhang, K.; Guo, X.; Fu, S.; Ding, K.; Li, A. Experiments of cooling EGR temperature influence on emission of diesel engines of vehicles. *Trans. CSAE* **2009**, *25*, 127–130.

82. Du, X.W. Diesel Engine EGR Cooler Fouling Investigation. *Intern. Combust. Engine Parts* **2017**, *22*–25. https://doi.org/10.19475/j.cnki.issn1674-957x.2017.12.012.
83. Zhu, R.; Sun, W.; Du, J.; Li, L.; Li, G.; Li, W. Effects of EGR on Combustion and Emission Characteristics for Two-stage Turbocharged High-pressure Common Rail Diesel Engine. *Veh. Engine* **2014**, *73*–77+88. https://doi.org/10.3969/j.issn.1001-2222.2014.04.015.
84. Guan, W. Experimental Study on Performance Optimization of China Stage IV Diesel Engine Combustion System Based on EGR. Master's Thesis, Guangxi University, Nanning, China, 2015.
85. Feng, H.; Li, J.; Wang, X.; Yu, J. Development and Experimental Verification of CDPF Assisted Passive Regeneration Control Strategy. *Veh. Engine* **2022**, *15*–20. https://doi.org/10.3969/j.issn.1001-2222.2022.05.003.
86. Miyairi, Y.; Miwa, S.; Abe, F.; Xu, Z.; Nakasuji, Y. *Numerical Study on Forced Regeneration of Wall-Flow Diesel Particulate Filters*; SAE Technical Paper 2001-01-0912; SAE: Warrendale, PA, USA, 2001. https://doi.org/10.4271/2001-01-0912.
87. Ohno, K.; Taoka, N.; Furuta, T.; Kudo, A.; Komori, T. *Characterization of High Porosity SiC-DPF*; SAE Technical Paper 2002-01-0325; SAE: Warrendale, PA, USA, 2002. https://doi.org/10.4271/2002-01-0325.
88. Kurimoto Y.; Mishina R.; Kato K.; Aoki T.; Honda T.; Kaneda A.; Vogt C.D. *Next Generation Diesel Particulate Filter for Future Tighter HDV/NRMM Emission Regulations*; SAE Technical Paper 2022-01-0545; SAE: Warrendale, PA, USA, 2022. https://doi.org/10.4271/2022-01-0545.
89. Kitagawa, J.; Hijikata, T.; Makino, M. Effects of DPF Volume on Thermal Shock Failures during Regeneration; SAE Technical Paper 890173; SAE: Warrendale, PA, USA, 1989. https://doi.org/10.4271/890173.
90. Lee, S.J.; Jeong, S.J.; Kim, W.S. Numerical design of the diesel particulate filter for optimum thermal performances during regeneration, *Appl*. *Energy* **2009**, *86*, 1124–1135. https://doi.org/10.1016/j.apenergy.2008.07.002.
91. Fekete, N.; Mandel, R.; Meissner, R.; Sander, H.; Wenninger, G. Method for Determining Mass of Soot Arranged in Particle Filter in Exhaust Gas System of Internal Combustion Engine, Involves Determining Parameter of Particulate Filter Laden with Soot Using Particulate Specific Input Size. Germany DE102008014509A1, 19 February 2009. Available online: https://patents.google.com/patent/DE102008014509A1/en (accessed on 1 September 2024).
92. Nakamura, K.; Vlachos, N.; Konstandopoulos, A.; Iwata, H.; Kazushige, O. *Performance Improvement of Diesel Particulate Filter by Layer Coating*; SAE Technical Paper 2012-01-0842; SAE: Warrendale, PA, USA, 2012. https://doi.org/10.4271/2012-01-0842.
93. Ogyu, K.; Yamakawa, T.; Ishii, Y.; MInoura, D.; Nagatsu, Y.; Kasuga, T.; Ohno, K. *Soot Loading Estimation Accuracy Improvement by Filtration Layer Forming on DPF and New Algorithm of Pressure Loss Measurement*; SAE Technical Paper 2013-01-0525; SAE: Warrendale, PA, USA, 2013. https://doi.org/10.4271/2013-01-0525.
94. Obata S.; Furuta Y.; Ohashi T.; Aoki T. *Gasoline Particulate Filter with Membrane Technology to Achieve the Tight PN Requirement*; SAE Technical Paper 2023-01-0394; SAE: Warrendale, PA, USA, 2023. https://doi.org/10.4271/2023-01-0394.
95. Aravelli, K.; Heibel, A. *Improved Lifetime Pressure Drop Management for Robust Cordierite (RC) Filters with Asymmetric Cell Technology (ACT)*; SAE Technical Paper 2007-01-0920; SAE: Warrendale, PA, USA, 2007. https://doi.org/10.4271/2007-01-0920.
96. Konstandopoulos, A.G.; Zarvalis, D.; Kladopoulou, E.; Dolios, I. *A Multi-Reactor Assembly for Screening of Diesel Particulate Filters*; SAE Technical Paper 2006-01-0874; SAE: Warrendale, PA, USA, 2006. https://doi.org/10.4271/2006-01-0874.
97. Nakano, K.; Okano, H.; Inoue, K.; Obuchi, A. *Study on the Prevention of Face-Plugging of Diesel Oxidation Catalyst (DOC)*; SAE Technical Paper 2018-32-0069; SAE: Warrendale, PA, USA, 2018. https://doi.org/10.4271/2018-32-0069.
98. Yang, K.; Fox, J.T.; Hunsicker, R. Characterizing Diesel Particulate Filter Failure During Commercial Fleet Use due to Pinholes, Melting, Cracking, and Fouling. *Emiss. Control Sci. Technol*. **2016**, *2*, 145–155. https://doi.org/10.1007/s40825-016-0036-0.
99. Ragaller, P.; Sappok, A.; Bromberg, L.; Gunasekaran, N.; Warkins, J.; Wilhelm, R. *Particulate Filter Soot Load Measurements using Radio Frequency Sensors and Potential for Improved Filter Management*; SAE Technical Paper 2016-01-0943; SAE: Warrendale, PA, USA, 2016. https://doi.org/10.4271/2016-01-0943.
100. Joshi, A.; Chatterjee, S.; Sawant, A.; Akerlund, C.; Andersson, S.; Blomquist, M.; Brooks, J.; Kattan, S. *Development of an Actively Regenerating DPF System for Retrofit Applications*; SAE Technical Paper 2006-01-3553; SAE: Warrendale, PA, USA, 2006. https://doi.org/10.4271/2006-01-3553.
101. Boger, T.; Rose, D.; Tilgner, I.; Heibel, A. Regeneration Strategies for an Enhanced Thermal Management of Oxide Diesel Particulate Filters. *SAE Int. J. Fuels Lubr.* **2009**, *1*, 162–172. https://doi.org/10.4271/2008-01-0328.
102. Miao, L.; Chen, C. Experimental Study on Drop-to-Idle During Diesel Particulate Filter Active Regeneration Process. *Moden Veh. Power* **2020**, *25*–29. https://doi.org/10.3969/j.issn.1671-5446.2020.04.006.